# LABORATORY SCALE EVALUATION OF COMPLIANT DRILLSTRING WITH PDC BITS IN GEOTHERMAL APPLICATIONS

By

LAYMON BARNETT

Bachelor of Science in Biosystems Engineering

Oklahoma State University

Stillwater, Oklahoma

2022

Submitted to the Faculty of the
Graduate College of the
Oklahoma State University
in partial fulfillment of
the requirements for
the Degree of
MASTER OF SCIENCE
May, 2022

LABORATORY SCALE EVALUATION OF COMPLIANT DRILLSTRING WITH PDC BITS IN GEOTHERMAL APPLICATIONS

Thesis Approved:

Dr. Mohammed F. Al Dushaishi

---

Thesis Adviser

Dr. Geir Hareland

---

Dr. Prem Bikkina

---

ACKNOWLEDGEMENTS

I first want to thank my committee members and professors, beginning with my advisor, Dr. Mohammed Al Dushaishi. As well as Dr. Geir Hareland and Dr. Prem Bikkina.

I would like to thank the U.S. Department of Energy, Office of Energy Efficiency & Renewable Energy, under Award Number EE0008603, for supporting this research. Additionally, I would like to thank National Oilwell Varco for their support. I also wish to thank Sandia National Laboratories for allowing the testing to be performed at their Hard Rock Drilling Facility, and specifically David W. Raymond of the Sandia team for facilitating that teamwork.

Name: LAYMON BARNETT

Date of Degree: MAY, 2022

Title of Study: LABORATORY SCALE EVALUATION OF COMPLIANT DRILLSTRING WITH PDC BITS IN GEOTHERMAL APPLICATIONS

Major Field: PETROLEUM ENGINEERING

Abstract: Polycrystalline diamond compact (PDC) bits have shown tremendous performance compared to roller cone bits and have gained attraction in deep geothermal drilling applications. While PDC bits can reach a higher rate of penetration compared to other bit types, they are more prone to drilling vibrations, especially torsional vibrations. Drillstring vibrations are one challenge that hinders efficient drilling and causes downhole tool failures. The objective of this work is to investigate the effects of drillstring vibrations on drilling performance by utilizing a laboratory testing facility. The test facility is equipped with an advanced drillstring simulator using suspension and torsional springs systems mimicking the natural vibrations modes of a field drillstring. Drilling tests were performed with various drillstring configurations which include rigid, flywheel, torsional compliance, axial compliance, and combined axial-torsional compliance. Two 3¾ inches PDC bits, with different designs, were used to evaluate the different drillstring vibration modes' effect on the bits' rate of penetration and output torque. The drilling tests were conducted at three constant rotational speeds of 80, 120, and 160 RPM, and the axial load varied by approximately 500 lb increments from 1500-5500 lb. The testing results from torsional compliance testing showed decreased performance relative to the rigid drillstring results by a margin of 35%. Additionally, the torsional compliance configuration facilitates more stable torque, and thus superior drilling over the rigid configuration when both configurations are in the inefficient phase. The axial compliance drillstring maintains a 5-20% margin of improved performance over the combined axial-torsional compliance in the 4-blade testing. The results of the 5-blade bit in axial compliance showed superior performance compared to the combined compliance by 17%, 38%, and 65% for the 80, 120, and 160 RPM tests, respectively. Overall, the experimental results showed that drillstring compliance configurations enhance drilling performance at the low weight on bit (WOB), during inefficient drilling, and decrease the drilling performance in the efficient drilling phase, i.e. high WOB.

TABLE OF CONTENTS

LIST OF TABLES

LIST OF FIGURES

CHAPTER I

# 1 INTRODUCTION

The cost of drilling a well, either for geothermal or oil and gas utilization, is high due to the time spent drilling hard formations with a slow penetration rate (ROP) and due to non-productive time. For geothermal wells, the return on investment is not as high as in oil and gas wells, where drilling cost plays a major role in the overall investments in geothermal energy. Thus, it is in the interest of operators and service organizations to optimize drilling performance to most efficiently and effectively drill a well. Drilling technologies from the oil and gas industry have made their influence in geothermal drilling due to their effectiveness in increasing drilling performance, namely the rate of penetration. Polycrystalline diamond compact (PDC) bits revolutionized the US shale industry, and they have begun to show their effectiveness in hard rock applications as well, such as those experienced in geothermal drilling.

While PDC bits are widely accepted to produce higher rates of penetration over their roller cone counterparts, it is also recognized that they can be more susceptible to drillstring vibrations, especially torsional vibrations. It is generally accepted that in most instances, drillstring vibrations negatively affect drilling performance. What remains to be seen however in the current literature, is the extent to which performance is affected. Laboratory scale testing has been done with PDC bits in numerous variations, which will be later discussed in further detail in the literature review.

However, oftentimes these studies don’t effectively account for the effect of drillstring vibrations. To account for the effect of drillstring vibrations in laboratory settings, the drillstring configuration is modified to mimic the natural frequencies of a field drillstring rather than using a rigid drillstring with much higher natural frequencies that are typically used. This particular study encompasses the performance of a rigid drillstring, as well as a drillstring that is torsionally and/or axially compliant, meaning that the laboratory drillstring's natural frequencies are reduced to match the field's natural frequency in the axial and torsional directions.

The scope of this work is to quantify to what extent drillstring vibrations affect drilling performance. To achieve this goal, compliant drillstring testing was done at Sandia National Laboratories’ (SNL) Hard Rock Drilling Facility (HRDF), where two PDC bits with different designs were used with Sierra White Granite rock samples.

CHAPTER II

# 2 LITERATURE REVIEW

Drillstring vibrations are complex due to the bottomhole assembly (BHA) design and the multiple forces acting on the drillstring such as drillstring contact with the wellbore wall and drill bit interaction with the formation rock. Such factors also affect drilling performance, specifically the drill bit interaction which is a function of the bit design and the formation lithology. The following literature review will discuss previous studies pertaining to drilling performance measurements and evaluation, drilling vibrations and their impact, and previous laboratory studies addressing PDC bits.

## 2.1 Drilling Performance Evaluation

Drilling rate, i.e. ROP, for a specific drill bit design is a function of the bit design aggressiveness, the rock strength, the applied WOB, and rotation per minute (RPM). For efficient drilling, the bit should exhibit a proportional increase in ROP due to an increase in WOB and rotational speed. When ROP is not proportional to the change of WOB or rotational speed, the drill bit is drilling inefficiently due to a certain dysfunction, hindering the optimum depth of cut (DOC). Regardless of bit design and rock strength, ROP should have a constant slope with the applied WOB when the bit is drilling efficiently. For example, Figure 2.1 shows the ROP response versus WOB for different scenarios. Changing the RPM for a specific bit design will change the slope relationship between the ROP and WOB while having a proportionate response (Figure 2.1a). Similar behavior will be seen with drilling a soft rock versus a hard rock (Figure 2.1b) and using an aggressive bit versus a less aggressive bit (Figure 2.1c).

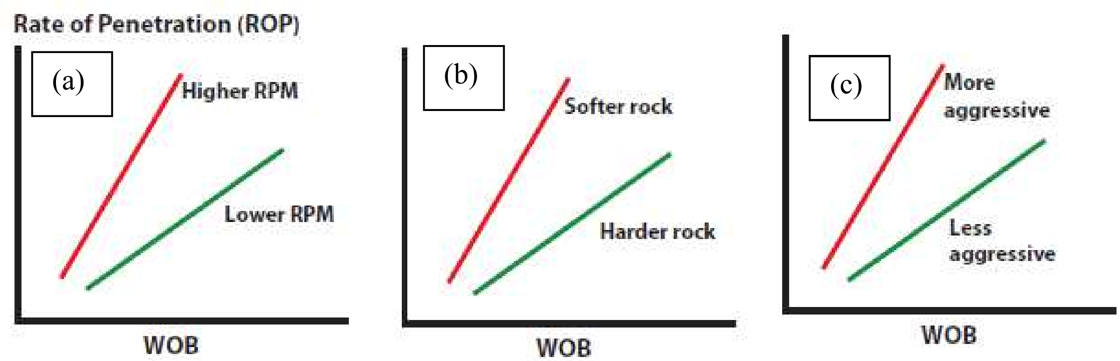


*Figure 2.1. Bit Response in Efficient Drilling Due to the Change of (a)RPM (b)Rock Hardness (c)Bit Aggression (IADC Drilling Manual, 12th Edition, 2014)*

As the bit tags bottom with low WOB, the bit tends to drill inefficiently, whereas increasing WOB raises that efficiency (Figure 2.2 (a)). At point 1 in Figure 2.2 (a), the peak efficiency is reached and stays constant with increasing WOB with a linear increase in ROP till it reaches point 2, which is known as the founder point. Increasing WOB beyond the founder point will cause a drop in ROP due to insufficient hole cleaning or bit balling. Increasing the flow rate will extend the limit of the founder point allowing for higher ROP as seen in Figure 2.2 (b).

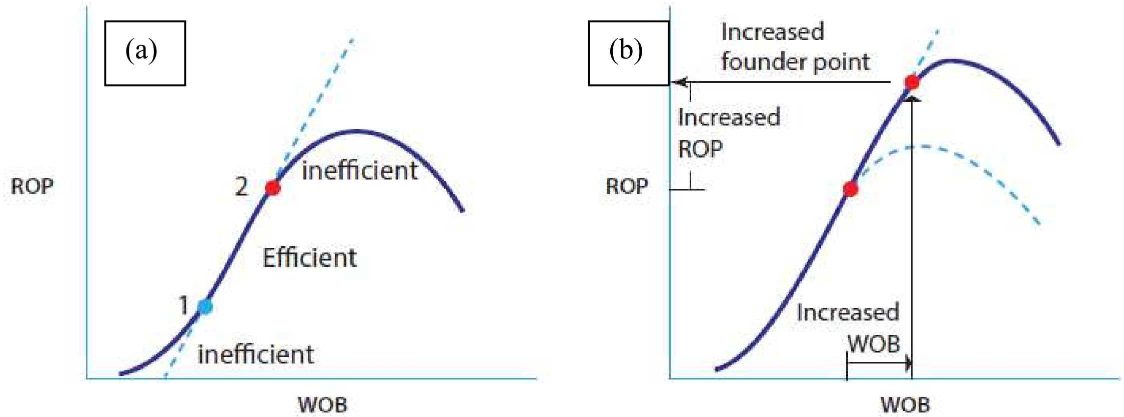


*Figure 2.2. ROP vs WOB Response Curve (a) Inefficient and Efficient Drilling Limits, (b) Founder Point Manipulation (IADC Drilling Manual, 2014)*

The founder point and bit performance are normally determined in the field using the drill-off test. In this test, the driller applies the WOB to a predetermined maximum load, normally close to the bit allowable limit, and then locks the top-drive position. The bit drill ahead and WOB decreases and as a result the hookload increases and cause the drillstring to elongate. The rate at which the hookload increases indicates how fast the drillstring is elongating, which is used to obtain the bit ROP (IADC Drilling Manual, 2014).

The mechanical specific energy (MSE), developed by Teale (1965), is another surveillance method for measuring drilling efficiency. The MSE is defined as the amount of work required to remove a volume of rock and can be calculated in psi, based on the drilling parameters according to:

$$MSE = \frac{480 \times T \times RPM}{{D_b}^2 \times ROP} + \frac{4 \times WOB}{\pi \times {D_b}^2} \tag{1}$$

Where T is torque measured in ft.lb, $D_b$ is the drill bit diameter in inches, ROP is the rate of penetration in ft/hr, and the weight on bit (WOB) is measured in lbf. The MSE allows for a continuous calculation of the amount of work the bit is doing and can be used to evaluate if the bit is drilling efficiently as the MSE changes with the change of operating parameters. The MSE by itself is used in the field as a relative indicator since the rock strength is generally unknown while drilling. A low MSE value indicates efficient drilling, while a high MSE value indicates inefficient drilling.

In theory, the MSE value should be equal to the rock strength when drilling efficiently. Dupriest and Koederitz (2005) modified the MSE equation developed by Teale (1965) using an adjusted MSE value ($MSE_{adj}$) that takes into consideration a mechanical efficiency factor because bits are typically 30-40% efficient at peak performance. It was shown that bit balling, bottom hole balling, and bit dulling can show distinct trends in real-time MSE monitoring. However, in practice, it's much more difficult to identify vibrations as the primary cause of inefficiency when all other factors are in play, and even more so, what kind of vibrations are occurring (Dupriest and Koederitz, 2005).

## 2.2 Hard Rock And Geothermal Drilling Challenges

Some of the common rock types in geothermal reservoirs are granite, granodiorite, quartzite, and basalt. Compared to oil and gas sedimentary formations, geothermal formations are hot, hard, abrasive, highly fractured, and under-pressured (Finger and Blankenship, 2010). With these conditions, geothermal drilling is usually difficult due to the slow ROP, short bit life, and severe lost circulation. In general, geothermal drilling is more expensive than onshore oil and gas drilling due to well design, which requires larger hole sizes, the requirement of special downhole tools that can handle high temperatures, bit life as it requires more frequent tripping which increases the cost per foot, and limitation on directional drilling technologies. Additionally, a very low quantity of geothermal wells, relative to oil and gas wells, has resulted in a lack of encouragement to actively seek drilling improvements. With respect to PDC bits specifically, their high initial cost relative to roller cone bits plays into that hand as well. However, it has since been shown that commercial off-the-shelf PDC bits have the capability to drill geothermal wells at higher ROPs and longer bit lifetimes than the traditional roller cones typically used. Although, the susceptibility of PDC bits to torsional vibrations is apparent while drilling, and that factor needs to be considered in planning

(Raymond et. al, 2012). BHA design plays a significant role in the mitigation of these vibrations, as well as bit design as a more aggressive bit will require higher rig torque capabilities to overcome the torsional influences of the wellbore (Barnett et. al, 2021).

The use of PDC bits in the oil and gas industry has gained popularity due to their higher ROP and drillability (Hareland et al., 2009). Traditionally, however, PDC bits showed poor performance in hard formations, such as formations encountered in geothermal applications. Extensive work has been performed to address PDC bit performance and its applicability in hard rock (Glowka and Stone, 1985; Raymond, 2001; Hareland et al., 2009; Raymond et al., 2012; Miyazaki et al., 2019; Rahmani et al., 2020; Akhtarmanesh et al., 2021; Atashnezhad et al., 2021).

Hareland et al., (2009) investigated the efficiency of a single PDC cutter on hard rock and concluded that cutters produce maximum efficiency at back rake angles of 0° and 25°when drilling hard rock. The effect of cutter geometry and the diamond table material composition of PDC bits in hard rock was addressed to support the development of PDC bits in hard rock (Wise et al., 2002). Their study indicated that the performance of PDC bits can be improved for hard rock drilling. Miyazaki et al., (2019) evaluated the effect of formation strength on PDC bit performance in hard rock. Their experiments indicated that PDC bit wear is highly affected by the rock unconfined compressive strength (UCS) and directly related to the cutter wearflat length.

Wise et al., (2005) performed a series of field tests using PDC bits in hard rock using downhole diagnostic while drilling downhole tool in Catoosa Test facility. They compared several conventional PDC bits performance and showed that using diagnostic while drilling with feedback control can extend bit life and increases ROP in hard rock interval. Raymond et al., (2012) demonstrated the abilities of conventional PDC bits in drilling deep geothermal wells. The performance of two PDC bit runs was compared with a conventional geothermal roller-cone bit run, where the PDC bits indicated longer lifetimes and higher ROP. Their field demonstration indicated that a PDC bit with impact arrestors aid in reducing drill bit vibrations.

The effect of confining pressure on ROP and MSE has been studied in recent years, with studies reporting that an increase in confining pressure has a significant effect on MSE, namely an increase in MSE of three times that of atmospheric testing at 250 psi confining pressure in Carthage marble, Torrey Buff sandstone and Mancos shale (Rajabov et. al, 2012). Additionally, Rafatian et. al., (2010) reported that confining pressures as low as 150 psig can increase MSE significantly and reduce cutting efficiency by half in Carthage marble and Indiana limestone. Figure 2.3 below shows the single-cutter high-pressure testing facility at the University of Tulsa, which was utilized in both the Rajabov and Rafatian (2012 and 2010) experiments referenced above.

*Figure 2.3. High-Pressure Single-Cutter Testing Facility at the University of Tulsa (Rajabov et. al, 2012)*

ROP models have been studied for decades, with the intent to predict drilling performance and evaluate bits to be used in a particular application. Most ROP models are formation specific, where model accuracy is highly affected by the formation being drilled. Several ROP models were developed for PDC bits for different sedimentary rock formations. Hareland and Rampersad (1994) developed a PDC model based on single cutter interaction, lithology coefficient, and bit wear. Their model was scaled for a full PDC bit using the equivalent bit radius method. Several other PDC models (Motahhari et al., 2010; Kerkar et al., 2014) were developed based on single cutter interaction for sedimentary rocks by integrating operational parameters, bit design details, bit hydraulics, and bit wear.

Due to the unique challenges in geothermal drilling, it is imperative to develop models to predict ROP specifically designed for these types of rocks. Atashnezhad et al., (2020) developed an ROP model for PDC bits in hard rocks and integrated the wear flat area and interfacial friction angle in their ROP model. Using laboratory testing, Akhtarmanesh et al., (2021) developed an ROP model for geothermal application and included the effect of bit wear. Their model was verified with field data of two PDC bits.

## 2.3 Drillstring And Drilling Vibrations

Drillstring and drill bit vibrations pose challenges that could affect drill bit performance, such as poor drilling rate (Elsayed and Raymond, 2002), and could lead to failure of the bottom hole assembly (BHA) (Arevalo and Fernandes, 2012; Rivas et al., 2021; Albdiry and Almensory, 2016) and accelerate bit wear or even damage the bit (Al-Enezi et al., 2018, Al Dushaishi et al., 2018). While drilling, the drillstring exhibits axial, torsional, and lateral vibrations (Figure 2.4) that could lead to drill bits and BHA components failures. Axial vibrations generally result in a phenomenon called bit-bouncing, which can cause significant damage to the PDC cutters and bit as a whole (Ashley et al., 2001). This is more prevalent in vertical sections, where the axial vibration modes tend to disperse themselves as inclination builds. Torsional vibrations tend to manifest as stick-slip. This is where the torque on the bit, due to the contact friction with the rock, causes the bit to momentarily stick until the buildup torque above the bit overcomes the frictional forces and breaks the bit free, i.e. slip. This phenomenon results in temporary excessive rotational speed of the bit, which can potentially over-torque the BHA connections, or potentially cause drillstring twist-offs (Ashley et al., 2001). Lateral vibrations occur when the rotation of the BHA is eccentric, causing a side impact with the wellbore. From a bit type point of view, roller cone bits are known for generating axial vibrations, while PDC bits are known to generate stick-slip, bit whirl, and torsional resonance which play a significant factor in PDC bit's performance (Warren and Oster, 1998).

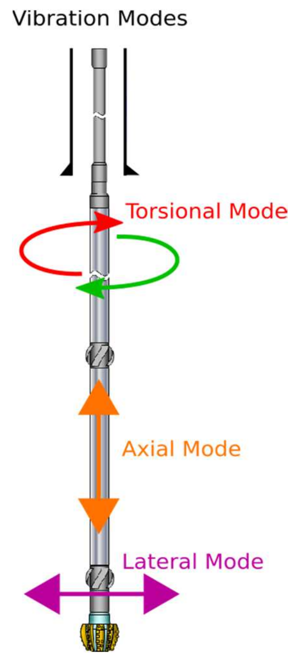


*Figure 2.4. Drillstring Vibration Modes (Barnett et. al, 2021)*

One of the key factors in optimizing the drilling process is maximizing ROP. Generally, operators attempt to do this by adjusting the WOB and RPM while drilling. However, there are many reasons including but not limited to: bit type, rock type, fluid type, and rig capabilities, that can dramatically affect the drilling process, i.e. may increase ROP but drastically reduce the bit and/or BHA life.

Drillstring vibrations can be measured at the surface or downhole. At the surface, rigs are outfitted with sensors in the top drive and drawworks that will measure parameters such as surface RPM, torque, and the applied WOB. Downhole tools such as measurement/logging while drilling (M/LWD) tools are equipped with a suite of sensors that, among other measurements, can measure vibration magnitude. These types of measurements can provide data in real-time, as well as more precise, i.e. higher resolution, in-memory mode.

Torsional vibrations, mainly stick-slip, are an extensively studied mode of drillstring vibrations. Generally, reducing the WOB for a given RPM or increasing the RPM for a given WOB will decrease the stick-slip severity (Richard et al., 2002). However, that's not always the case due to other factors such as BHA and bit designs, the formation being drilled, and the coupling between other vibration modes. PDC bits are prone to stick-slip vibrations which could lead to bit damage (Ledgerwood et al., 2013). Using numerical methods, Makkar et al., (2014) simulations suggest that as the drill bit transitions to unstable drilling, the lateral acceleration increases as well as the MSE.

Traditionally, drillstring vibrations have been known to cause reduced ROP or bit/BHA damage, however, the effect of drillstring vibrations on performance is addressed in two forms in the literature. The first form consists of using induced drilling vibration to improve ROP (Li et al., 2010; Babatunde et al., 2011; Clausen et al., 2014; Alwaar et al., 2018), while the second form consists of studying the effect of self-excited vibrations of the drilling assembly and the bit by determining critical operating conditions (Dunayevsky et al., 1993; Dunayevsky et al., 1998; Bailey et al., 2008; Feauto et al., 2013; Al Dushaishi et al., 2016).

## 2.4 Research Justification

The effect of drillstring vibrations on PDC drilling performance, specifically ROP, is not fully understood yet due to two main challenges. The first challenge is the complexity of the drilling dynamics due to the nonlinear forces acting on the drillstring such as the bit rock interaction and drillstring contacts with the wellbore wall. The second challenge is the inability to mimic actual drillstring dynamics in laboratory settings in a controlled environment. Many laboratory-scale experiments were conducted using a much stiffer drilling assembly than the actual field (Garcia-

Gavito and Azar, 1994; Miyazaki et al., 2019). While these types of setups are applicable for testing bit response to drilling forces and bit rock interactions, the actual dynamics due to the slender drillstring is not being considered. Previous studies of percussive drilling mainly addressed the effect of axial vibrations and a resultant increase in ROP due to those axial vibrations (Li et al., 2010; Clausen et al., 2014; Alwaar et al., 2018). However, the effect of solely torsional vibration has not been linked to ROP. The effect of combined axial-torsional vibrations on ROP has been addressed in several studies (Akutsu et al., 2015; Vromen et al., 2019). These studies showed that these mechanisms, reliant on a torsional spring that contracts to reduce applied axial load at the bit, can increase ROP by reducing stick-slip severity.

Elsayed and Raymond (1999) addressed the challenge of reproducing the drilling dynamics of the drillstring by adding compliance to the drilling step to study PDC bit chatter. Elsayed and Raymond (2002) investigated the effect of torsional vibrations on the dynamic stability of the drilling system without addressing its influence on the resultant ROP. The possibility of reproducing the bit and drillstring dynamics on a laboratory scale using an actual bit rock interaction and implementation of a drillstring dynamic response has been presented by Raymond et al., (2008).

This work aims to conclude to what extent drillstring vibrations impact drilling performance with varying drilling parameters and bit designs. This will be done by establishing a baseline dataset with which to compare the results of subsequent drilling tests with compliant drillstrings. Evaluation of the differences and effects of parameters will provide the quantitative results for analysis.

CHAPTER III

# 3 METHODOLOGY

## 3.1 Experimental Setup

The Hard Rock Drilling Facility (HRDF, Figure 3.1) at Sandia National Laboratories was designed to be an accurate representation of field drilling conditions. Figure 3.1 (a) shows the entirety of the experimental setup, and Figure 3.1 (b) shows a rock sample underneath the rig. Figure 3.1 (c) shows a simple schematic illustration of the HRDF. The rig consists of a drillstring that is supported by a hydraulically powered, vertically traversing frame that supports a rotating top drive system. The drillstring is rotated by a fixed-displacement hydraulic motor, and hydraulic cylinders apply an axial load to the drillstring, which is measured via the differential pressure across the cylinders. A swivel feeds water, as the drilling fluid, which is placed above the top drive. The rig is capable of testing drill bits with a diameter of up to 3 ¾ inches, with maximum weight on bit (WOB) and rotational speed of 5500 lbs and 160 RPM, respectively.

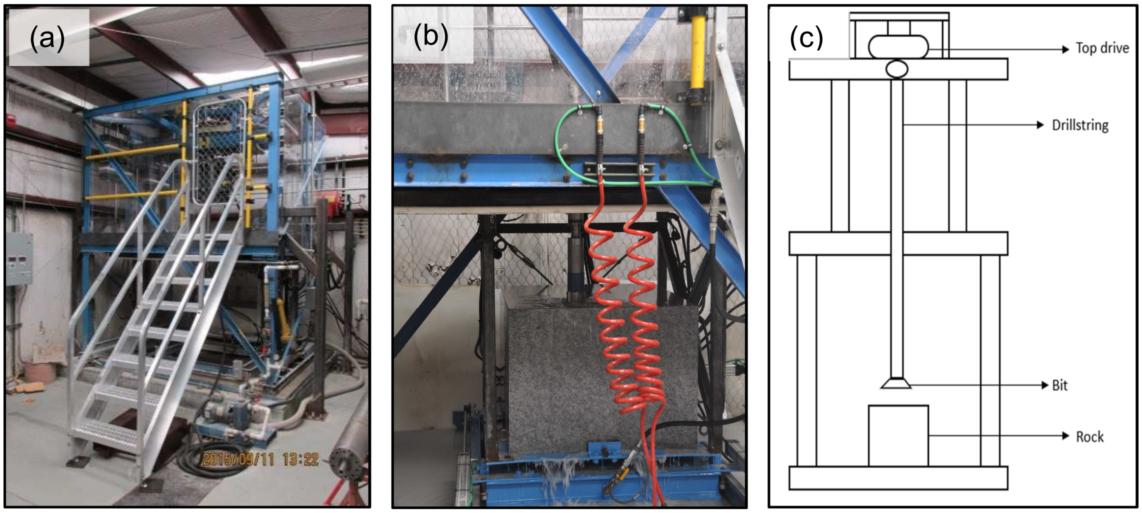


*Figure 3.1. (a) Drilling Facility, (b) Rock Sample, and (c) Schematic Illustration*

The rig is fully instrumented to monitor and control the drilling process and the bit response. The data acquisition system measures the rate of penetration (ROP), WOB, rotary speed, torque, and axial and torsional accelerations. The drill bit response is measured with a centerline position displacement transducer and a torsional position displacement transducer. A full description of the system is outlined by Raymond et al., (2008).

To measure the vibrational effects on drilling performance, five different test configurations were compared including; rigid, flywheel, torsional compliance, axial compliance, and combined axial-torsional compliance. The rigid configuration, without imposed vibration, is the common method of testing drill bit performance in a laboratory scale, which is used as a testing baseline. In field conditions, the drillstring natural frequencies are very low due to the drillstring slenderness ratio (Elsayed and Raymond, 2002; Raymond et al., 2008). Typical laboratory rigs are rigid with a much higher frequency range than the actual drillstring used in the field, hindering the investigation of several dynamic phenomena such as bit chatter. To address this issue, the flywheel configuration is used to increase the mass moment of inertia, which reduces the drillstring frequency to the field condition range. The flywheel configuration consists of a 24-inch diameter with a one-inch thick

A-34 steel plate mounted on the drillstring, referred to as a flywheel, to investigate the rotary mass moment of inertia effect on the drill bit response.

The torsional compliance configuration addresses the torsional direction of the field drillstring flexibility. The HRDF drillstring's torsional compliance capabilities are facilitated by two counter-wound springs. The springs are pre-loaded to ensure non-zero torque while winding and unwinding during drilling (Elsayed and Raymond, 2002). The torque and deflection relationship of the effective torsional springs is expressed as

$$\mathrm{T} = 123.13 * \theta + 85.507 \tag{3}$$

where T is torque response in lb-in and $\theta$ is the angular deflection in degrees.

Central computer monitors and records data including WOB, the left and right cylinder positions, torque, rotary speed, left and right spring compression, torsional deflection, and torsional acceleration. A transducer called the Torsional Position Displacement Transducer (TPDT) measures the torsional vibration in the drillstring relative to the drillstring's supporting structure (Elsayed and Raymond, 2002).

The axial compliance is facilitated by supporting the drillstring with a spring suspension system. Since both methods of compliance can independently be turned to rigid status, it was possible to perform combined compliance testing where both the axial and torsionally compliant methods were active. This combined compliance mode was utilized for the fifth test. Elsayed and Raymond (2002) present information on the HRDF in further detail.

Two PDC drill bits with different designs having a diameter of 3 ¾ inches were used. The first bit is a 4-blade PDC bit with a total of 15 primary cutters with diameters of 13 mm (Figure 3.2). The second PDC bit is a 5-blade design with 19 primary cutters with an 11 mm cutter diameter (Figure 3.3). Both bits were tested in Sierra White Granite, which has an unconfined compressive strength of 28,000 psi. Water was used as the drilling fluid, where a constant flow rate of 15 gallons per minute was used. The purpose of utilizing two different drill bits is to evaluate the drillstring configuration effect on different bit designs.


*Figure 3.2. Profile of the 4-Bladed PDC Bit Design*


*Figure 3.3. Profile of the 5-Bladed PDC Bit Design*

## 3.2 Data Preparation and Analysis

Each test was performed at a constant rotational speed and incremental axial load. The raw data from the SNL testing were measured with a sampling frequency of 512 samples per second. The test data consisted of a large .txt file that was generated from the testing (Table 3.1).

*Table 3.1. Raw SNL Data*

NOV 4-Blade Bit @ 80 RPM & WOB: 2000-5000 lb

Test # = 1 Hole # = 1 Hole Index = G2 Test Operator = David Control Mode = Constant WOB Control Target Value = 30

Test Time Time Pressure - top left Pressure - bottom left Pressure - top right Pressure - bottom right Axial Acceler

| | | | | | | | | |
|---|---|---|---|---|---|---|---|---|
| 0.0000 | 10:40:07 | 8.4902E+1 | 2.4564E+2 | 6.6082E+1 | 2.3352E+2 | 1.0175E-4 | -4.2939E-4 | -2.5801E-4 |
| 0.0020 | 10:40:07 | 8.4902E+1 | 2.4564E+2 | 6.6082E+1 | 2.3352E+2 | 7.7499E-5 | -1.5620E-3 | -1.3576E-3 |
| 0.0039 | 10:40:07 | 8.4902E+1 | 2.4564E+2 | 6.6082E+1 | 2.3352E+2 | 9.5037E-5 | -3.9148E-5 | 1.5986E-4 |
| 0.0059 | 10:40:07 | 8.4902E+1 | 2.4564E+2 | 6.6082E+1 | 2.3352E+2 | 1.1822E-4 | -2.3274E-3 | -2.1186E-3 |
| 0.0078 | 10:40:07 | 8.4972E+1 | 2.4523E+2 | 6.5842E+1 | 2.3335E+2 | 1.7632E-4 | -1.1175E-3 | -9.5020E-4 |
| 0.0098 | 10:40:07 | 8.4996E+1 | 2.4509E+2 | 6.5761E+1 | 2.3329E+2 | 1.3042E-4 | -2.2774E-3 | -2.0816E-3 |
| 0.0117 | 10:40:07 | 8.4996E+1 | 2.4509E+2 | 6.5761E+1 | 2.3329E+2 | 9.8697E-5 | -2.2063E-3 | -2.0174E-3 |
| 0.0137 | 10:40:07 | 8.4996E+1 | 2.4509E+2 | 6.5761E+1 | 2.3329E+2 | 1.3896E-4 | -8.9986E-4 | -7.4386E-4 |
| 0.0156 | 10:40:07 | 8.4922E+1 | 2.4525E+2 | 6.5740E+1 | 2.3328E+2 | 2.0774E-4 | -1.2053E-3 | -1.0395E-3 |
| 0.0176 | 10:40:07 | 8.4848E+1 | 2.4541E+2 | 6.5718E+1 | 2.3327E+2 | 1.9020E-4 | 5.1436E-5 | 2.4383E-4 |
| 0.0195 | 10:40:07 | 8.4848E+1 | 2.4541E+2 | 6.5718E+1 | 2.3327E+2 | 1.7708E-4 | -2.3960E-6 | 1.8912E-4 |
| 0.0215 | 10:40:07 | 8.4848E+1 | 2.4541E+2 | 6.5718E+1 | 2.3327E+2 | 1.9203E-4 | 1.7730E-3 | 1.9583E-3 |
| 0.0234 | 10:40:07 | 8.4917E+1 | 2.4531E+2 | 6.5737E+1 | 2.3323E+2 | 2.8460E-4 | 1.5019E-3 | 1.7009E-3 |
| 0.0254 | 10:40:07 | 8.5125E+1 | 2.4499E+2 | 6.5792E+1 | 2.3313E+2 | 3.3309E-4 | 5.6078E-4 | 7.3013E-4 |
| 0.0273 | 10:40:07 | 8.5125E+1 | 2.4499E+2 | 6.5792E+1 | 2.3313E+2 | 3.0763E-4 | 5.0979E-5 | 2.3636E-4 |
| 0.0293 | 10:40:07 | 8.5125E+1 | 2.4499E+2 | 6.5792E+1 | 2.3313E+2 | 2.7621E-4 | -7.3561E-4 | -5.4620E-4 |
| 0.0312 | 10:40:07 | 8.5125E+1 | 2.4499E+2 | 6.5792E+1 | 2.3313E+2 | 3.0900E-4 | -2.3908E-4 | -5.3193E-5 |
| 0.0332 | 10:40:07 | 8.5181E+1 | 2.4506E+2 | 6.5904E+1 | 2.3313E+2 | 3.0610E-4 | -2.4383E-3 | -2.2505E-3 |
| 0.0352 | 10:40:07 | 8.5181E+1 | 2.4506E+2 | 6.5904E+1 | 2.3313E+2 | 2.4113E-4 | -1.4630E-3 | -1.2652E-3 |
| 0.0371 | 10:40:07 | 8.5181E+1 | 2.4506E+2 | 6.5904E+1 | 2.3313E+2 | 1.9828E-4 | -2.1786E-3 | -1.9752E-3 |
| 0.0391 | 10:40:07 | 8.5181E+1 | 2.4506E+2 | 6.5904E+1 | 2.3313E+2 | 2.1582E-4 | 3.3875E-4 | 5.2073E-4 |
| 0.0410 | 10:40:07 | 8.5103E+1 | 2.4505E+2 | 6.5694E+1 | 2.3317E+2 | 2.0118E-4 | -3.7565E-3 | -3.5457E-3 |
| 0.0430 | 10:40:07 | 8.5076E+1 | 2.4505E+2 | 6.5624E+1 | 2.3318E+2 | 1.2295E-4 | -1.8017E-3 | -1.6343E-3 |
| 0.0449 | 10:40:07 | 8.5076E+1 | 2.4505E+2 | 6.5624E+1 | 2.3318E+2 | 9.1987E-5 | -2.3044E-3 | -2.1045E-3 |
| 0.0469 | 10:40:07 | 8.5076E+1 | 2.4505E+2 | 6.5624E+1 | 2.3318E+2 | 1.0373E-4 | -1.5782E-3 | -1.4097E-3 |
| 0.0488 | 10:40:07 | 8.4966E+1 | 2.4521E+2 | 6.5744E+1 | 2.3316E+2 | 1.3957E-4 | -4.8146E-5 | 1.4584E-4 |
| 0.0508 | 10:40:07 | 8.4856E+1 | 2.4537E+2 | 6.5865E+1 | 2.3313E+2 | 1.0373E-4 | 2.5609E-4 | 4.4012E-4 |
| 0.0527 | 10:40:07 | 8.4856E+1 | 2.4537E+2 | 6.5865E+1 | 2.3313E+2 | 3.4646E-5 | -9.8724E-4 | -8.1198E-4 |
| 0.0547 | 10:40:07 | 8.4856E+1 | 2.4537E+2 | 6.5865E+1 | 2.3313E+2 | 7.8109E-5 | -2.0924E-3 | -1.9348E-3 |
| 0.0566 | 10:40:07 | 8.4902E+1 | 2.4530E+2 | 6.5819E+1 | 2.3313E+2 | 9.8545E-5 | -2.4285E-3 | -2.2453E-3 |

A MATLAB code was generated to read the raw data .txt file, and since the data acquisition rate was 512 samples/second, every 512 samples were averaged to create a single data row per second. The code also cleaned the data, namely by deleting any rows with ROP, RPM, or WOB values of less than 0. Utilized the clean data, the code produced an Excel workbook for easy analysis and data visualization (Table 3.2).

*Table 3.2. Cleaned SNL Data*

| Time (s) | WOB (lbf) | RPM (rev/min) | Torque (lb-ft) | ROP (ft/hr) | Cyl. Pos. (in) | Specific Energy | Drilling Strength |
|---|---|---|---|---|---|---|---|
| 27 | 208.422009 | 65.25201367 | 38.41124674 | 20.48603125 | 3.17751182 | 3959.946875 | -2919.826563 |
| 28 | 595.078066 | 70.86663086 | 37.34053711 | 24.03215625 | 3.2584335 | 3697.953125 | 3999.355938 |
| 29 | 605.931133 | 73.00620312 | 37.4323112 | 24.33153125 | 3.34014404 | 3899.4375 | 4739.26875 |
| 30 | 602.619902 | 76.02972656 | 35.60421549 | 24.56653125 | 3.42210762 | 3814.28125 | 4929.25625 |
| 31 | 596.585 | 79.194375 | 37.16158529 | 24.531375 | 3.50412861 | 3955.98125 | 5045.271875 |
| 32 | 593.356914 | 81.30862109 | 37.75844564 | 24.59340625 | 3.58617656 | 4028.640625 | 5155.090625 |
| 33 | 590.567031 | 81.65851758 | 35.18131999 | 24.6330625 | 3.66766104 | 4090.7875 | 5266.40625 |
| 34 | 589.591621 | 81.92303125 | 34.78979004 | 24.41046875 | 3.74919941 | 4072.80625 | 5269.846875 |
| 35 | 591.137363 | 82.08677734 | 34.49323893 | 24.50859375 | 3.83156748 | 3974.54375 | 5268.34375 |
| 36 | 589.024922 | 81.65232617 | 34.82106445 | 24.72746875 | 3.91364434 | 3986.334375 | 5205.215625 |
| 37 | 583.741289 | 82.52683594 | 36.02705078 | 24.63728125 | 3.99577715 | 3983.353125 | 5199.809375 |
| 38 | 578.2025 | 81.95972656 | 34.90349284 | 24.62559375 | 4.07766484 | 3947.040625 | 5167.525 |
| 39 | 573.937227 | 82.17225195 | 34.26077962 | 24.5984375 | 4.15927637 | 3931.225 | 5137.1375 |
| 40 | 571.656816 | 82.36542773 | 35.31226237 | 23.60646875 | 4.22240732 | 4083.865625 | 5279.9375 |
| 41 | 576.672773 | 81.96363281 | 34.72629395 | 16.48421875 | 4.26146016 | 6025.571875 | 7895.871875 |
| 42 | 571.210684 | 82.69357422 | 34.15669759 | 11.74165625 | 4.29988301 | 8605.665625 | 10773.57813 |
| 43 | 565.183125 | 82.89246094 | 34.49777018 | 11.57584375 | 4.33876846 | 8428.9125 | 10750.21875 |
| 44 | 564.692129 | 82.79425781 | 35.06946126 | 11.6386875 | 4.377321 | 8347.1375 | 10711.6875 |
| 45 | 575.870098 | 82.87212109 | 35.27602865 | 11.558875 | 4.4117999 | 8446.90625 | 10717.625 |
| 46 | 600.395703 | 81.93119922 | 35.38940755 | 8.8485625 | 4.42966055 | 10991.58125 | 15217 |
| 47 | 555.32459 | 82.02025781 | 33.90647949 | 4.95581875 | 4.44231006 | 20483.0625 | 25774.40625 |
| 48 | 557.8575 | 82.54375977 | 36.14722982 | 3.726071875 | 4.45450596 | 27524.125 | 32579.90625 |
| 49 | 559.696113 | 82.24619531 | 36.82042155 | 3.6650625 | 4.46665 | 27179.1875 | 33347.0625 |
| 50 | 562.855859 | 81.70437305 | 36.61964681 | 3.63674375 | 4.47854521 | 27365.125 | 33915.96875 |

From this cleaned data the upcoming results and discussion are created and analyzed. The beginning of each test showed a WOB offset that registered on the sensors, even though the cylinder position revealed that the bit was not contacting the rock. This value was identified and subtracted from the measured WOB to provide an accurate WOB value. A similar procedure was performed for torque measurements, as there was an initial offset measured by the torque sensors as well.

Although all values were constantly changing due to the high sampling rate, when a WOB value was relatively “set”, those values were identified and separated. Each collection of WOB values was averaged to determine singular WOB and torque for the duration of the set WOB interval. The MSE was calculated for each interval using the drill bit diameter and the drilling operating parameter for each WOB step. The ROP was calculated via the cylinder travel measurements and the timestamps. This procedure resulted in 5-7 distinct collections of data, i.e. WOB level, for each test at a constant rotational speed.

CHAPTER IV

# 4 RESULTS

A primary goal of this work is to determine the effect of drillstring vibrations on drilling performance. This is being made possible by the compliant drillstring configurations available at the SNL HRDF. The following sections present the results of this testing in detail.

## 4.1 Rigid Drillstring Configuration

Table 4.1 shows the processed drilling data of the rigid baseline testing for the 4- and 5-bladed PDC bits. The processed data consists of the applied WOB and each rotary speed test, the resultant ROP, torque, and calculated MSE.

*Table 4.1. Rigid Configuration Drilling Data of the 4- and 5-Bladed Bits*

| RPM | 4 Bladed PDC Bit | | | | 5 Bladed PDC Bit | | | |
|---|---|---|---|---|---|---|---|---|
| | WOB (lbf) | ROP (ft/hr) | Torque (lb-ft) | MSE (ksi) | WOB (lbf) | ROP (ft/hr) | Torque (lb-ft) | MSE (ksi) |
| 80 | 1515 | 0.92 | 50 | 149 | 1528 | 0.8 | 45 | 148 |
| | 2017 | 1.98 | 81 | 112 | 2029 | 1.6 | 65 | 112 |
| | 2523 | 3.93 | 116 | 81 | 2532 | 3.3 | 89 | 75 |
| | 3021 | 7.52 | 160 | 58 | 3030 | 5.3 | 117 | 60 |
| | 3528 | 13.51 | 214 | 44 | 3537 | 8.2 | 144 | 48 |
| | 4021 | 21.61 | 271 | 35 | 4031 | 12.2 | 177 | 40 |
| | 4521 | 29.09 | 319 | 30 | 4530 | 17.3 | 212 | 34 |
| | 5023 | 35.00 | 361 | 29 | 1469 | 1.7 | 52 | 127 |
| 120 | 1508 | 2.0 | 63 | 129 | 1973 | 2.2 | 62 | 117 |
| | 2013 | 2.6 | 78 | 126 | 2474 | 4.4 | 86 | 80 |
| | 2516 | 5.0 | 110 | 90 | 2975 | 7.1 | 109 | 63 |
| | 3011 | 9.2 | 149 | 66 | 3484 | 11.0 | 137 | 51 |
| | 3515 | 16.3 | 197 | 50 | 3973 | 16.3 | 172 | 44 |
| | 4020 | 26.6 | 248 | 39 | 4476 | 22.8 | 202 | 37 |
| | 4527 | 38.0 | 298 | 33 | 4974 | 31.0 | 238 | 32 |
| | 5019 | 47.7 | 341 | 30 | 1517 | 4.3 | 67 | 84 |
| 160 | 1546 | 3.6 | 77 | 116 | 2018 | 3.4 | 71 | 113 |
| | 2055 | 3.4 | 79 | 128 | 2522 | 6.0 | 89 | 82 |
| | 2541 | 6.4 | 107 | 92 | 3019 | 9.1 | 110 | 66 |
| | 3060 | 10.5 | 139 | 72 | 3520 | 13.6 | 135 | 55 |
| | 3553 | 18.0 | 179 | 55 | 4017 | 20.1 | 164 | 45 |
| | 4065 | 29.3 | 227 | 43 | 4520 | 27.7 | 192 | 38 |
| | 4564 | 42.9 | 279 | 36 | 5016 | 37.4 | 225 | 33 |
| | 5071 | 55.0 | 321 | 32 | 1528 | 0.8 | 45 | 148 |

Figure 4.1 (a)-(c) shows the plotted data from the 80, 120, and 160 RPM tests showing ROP vs. WOB, Torque vs. WOB, and Torque vs. ROP, respectively. As visible on the ROP vs. WOB plot (Figure 4.1 (a)), for a given WOB at any of the tested RPMs, ROP is higher at a faster applied rotary speed. Additionally, Figure 4.1 (b) shows the torque versus WOB relationship, where generally lower torque is seen for higher RPM except at low WOB. At approximately 1500 lbf, higher RPMs result in lower torque, which could be due to the lack of bit rock interaction. Figure 4.1 (c) shows the correlation between ROP and torque, where it can be seen that higher torque is required to achieve a certain ROP as rotary speed decreases.

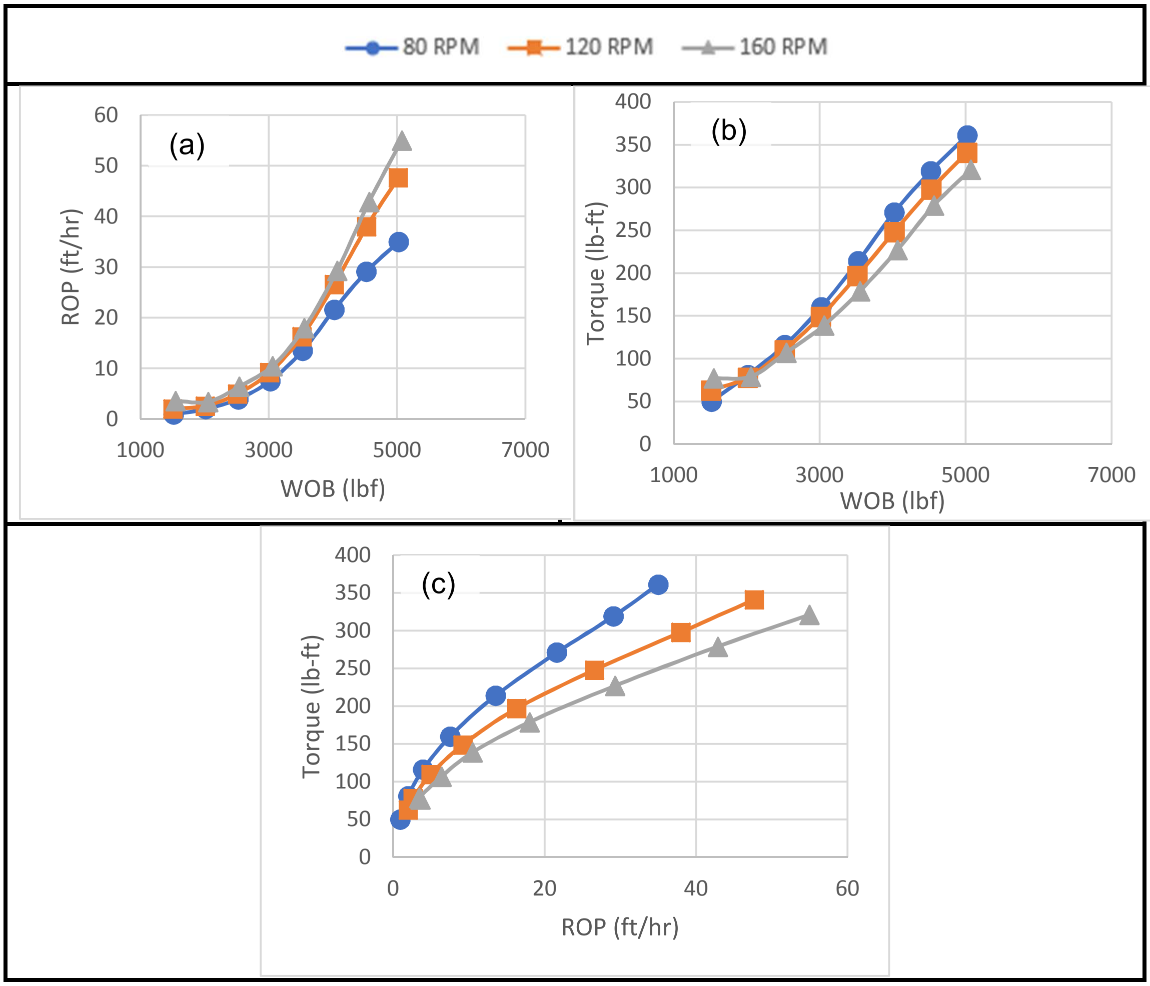


*Figure 4.1. Rigid 4-Bladed (a)ROP vs WOB, (b) Torque vs WOB, (c) Torque vs ROP*

All of the 5-blade curves (Figure 4.2) show similar trends and correlations to the 4-blade curves. The torque versus WOB relationship (Figure 4.2 (b)) shows that the first two data points agree with the initial data in Figure 4.1 (b) as far as resultant torque values. However, for a given WOB, after 2500lbf is reached the data produces lower torque values than the 4-bladed test. In general, the 5-bladed bit produces a lower ROP and torque range.

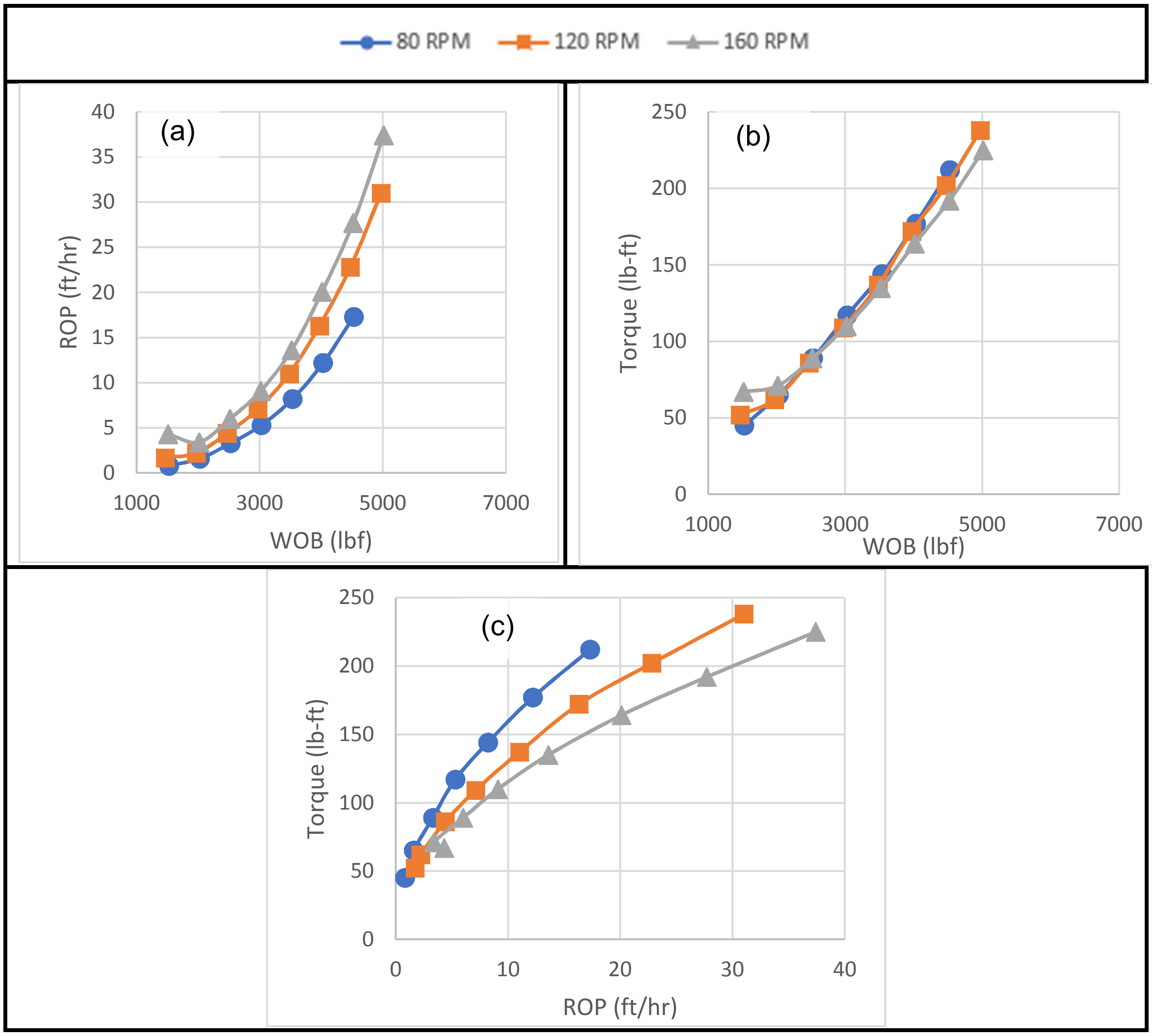


*Figure 4.2. Rigid 5-Bladed (a) ROP vs WOB, (b) Torque vs WOB, (c) Torque vs ROP*

## 4.2 Flywheel Drillstring Configuration

Table 4.2 shows the processed data from the 4- and 5-bladed PDC tests with the flywheel installed.

*Table 4.2. Processed Flywheel Data for 4- & 5-Bladed PDC Bits*

| RPM | 4 Bladed PDC Bit | | | | 5 Bladed PDC Bit | | | |
|---|---|---|---|---|---|---|---|---|
| | WOB (lbf) | ROP (ft/hr) | Torque (lb-ft) | MSE (ksi) | WOB (lbf) | ROP (ft/hr) | Torque (lb-ft) | MSE (ksi) |
| 80 | 1633 | 1.3 | 47 | 100 | 1642 | 1.1 | 45 | 112 |
| | 2133 | 2 | 84 | 114 | 2141 | 1.8 | 69 | 166 |
| | 2633 | 3.69 | 116 | 86 | 2641 | 3.4 | 90 | 108 |
| | 3131 | 6.1 | 151 | 68 | 3145 | 5.1 | 113 | 83 |
| | 3630 | 10.56 | 199 | 52 | 3641 | 7.7 | 140 | 66 |
| | 4139 | 18.86 | 260 | 38 | 4150 | 11.5 | 173 | 52 |
| | 4624 | 26.77 | 305 | 32 | 4647 | 14.9 | 198 | 45 |
| | 5144 | 35.38 | 360 | 28 | 5136 | 20 | 227 | 37 |
| 120 | 1617 | 3.1 | 53 | 70 | 1661 | 2.6 | 60 | 176 |
| | 2118 | 3 | 76 | 105 | 2170 | 2.5 | 67 | 192 |
| | 2617 | 5.1 | 106 | 86 | 2669 | 4.5 | 87 | 123 |
| | 3119 | 8.1 | 138 | 70 | 3171 | 6.7 | 107 | 95 |
| | 3626 | 13.2 | 179 | 56 | 3667 | 10.4 | 134 | 73 |
| | 4119 | 21.9 | 226 | 43 | 4168 | 14.5 | 160 | 61 |
| | 4628 | 33.1 | 279 | 35 | 4676 | 20.4 | 191 | 49 |
| | 5120 | 45.5 | 329 | 30 | 5171 | 27 | 221 | 41 |
| 160 | 1686 | 4.0 | 65 | 89 | 1680 | 5.1 | 74 | 132 |
| | 2184 | 3.4 | 83 | 133 | 2190 | 5.3 | 88 | 143 |
| | 2684 | 6.2 | 103 | 92 | 2693 | 5.4 | 92 | 141 |
| | 3185 | 9.4 | 129 | 75 | 3185 | 8.4 | 112 | 105 |
| | 3682 | 14.5 | 162 | 61 | 3688 | 12.3 | 134 | 84 |
| | 4182 | 22.1 | 204 | 51 | 4191 | 16.9 | 157 | 68 |
| | 4688 | 33.7 | 247 | 40 | 4688 | 22.3 | 180 | 58 |
| | 5196 | 49.4 | 302 | 34 | 5193 | 29.6 | 208 | 48 |

Figure 4.3 presents the plotted data from the testing for the rigid test with a flywheel installed to increase inertia. Generally, the testing with the flywheel installed averaged roughly 100 lbf higher in the WOB measurements for both 4 and 5 blade testing. The 80 RPM testing produced very similar ROP values to the previous rigid testing. The 120 RPM with the flywheel showed slightly lower ROP values throughout, and the 160 RPM test produced noticeably lower ROP values with the flywheel. For all rotational speeds, the differences are amplified at a higher WOB range. All correlations and trends were the same, with the largest discrepancy in Figure 4.3 (b) in the ROP

values where the 120 RPM and 160 RPM datasets maintain a difference of steady magnitude as opposed to increasing in separation. For each dataset, the 5-blade results (Figure 4.3 (d)-Figure 4.3 (f)) show similar trends, although with generally lower ROP throughout.

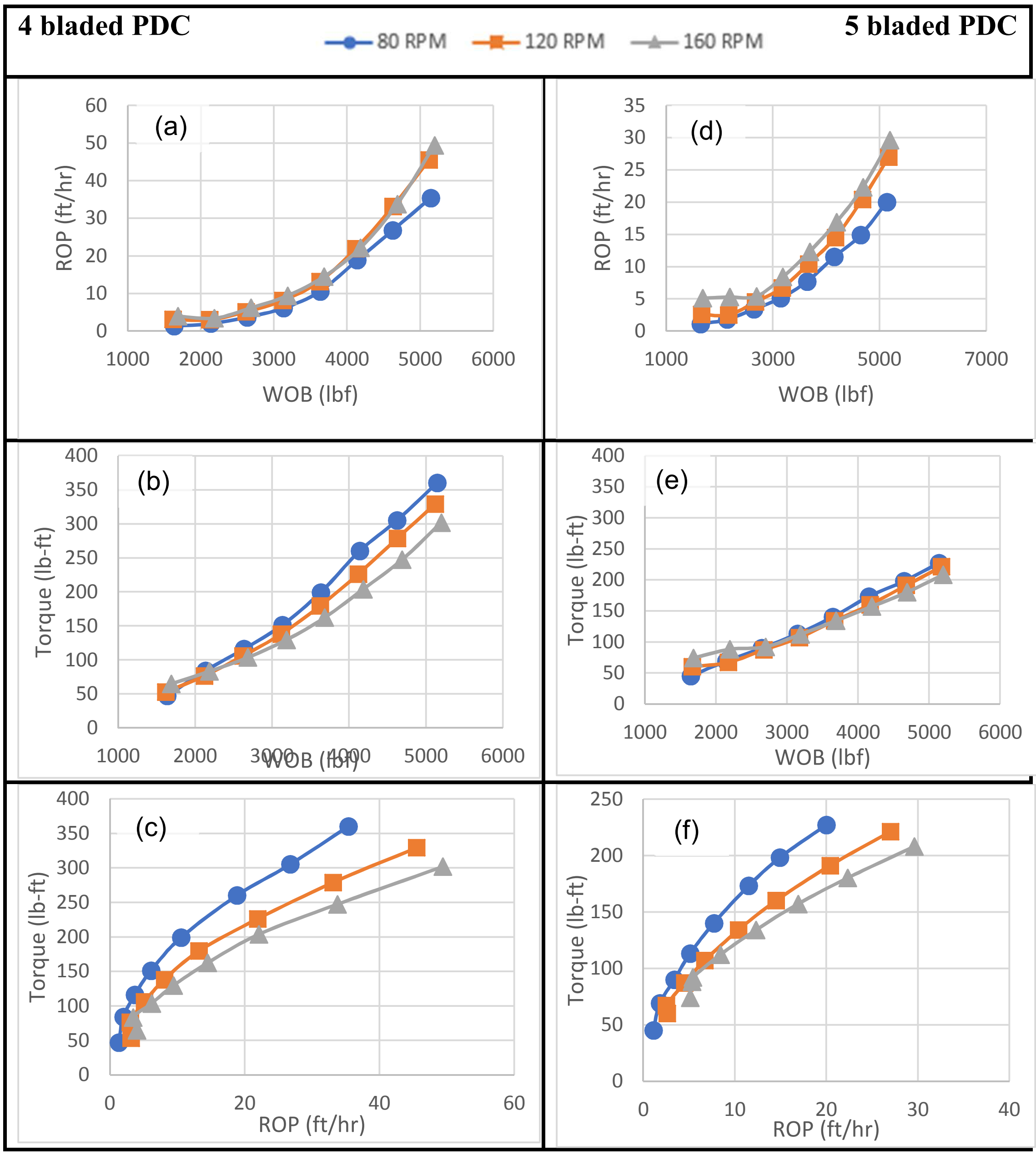


*Figure 4.3. Flywheel 4-Bladed ROP vs WOB (a), Torque vs WOB (b), Torque vs ROP (c); 5-Bladed ROP vs WOB (d), Torque vs WOB (e), Torque vs ROP (f)*

### 4.2.1 Flywheel and rigid configurations comparison

The flywheel test configuration was designed to reduce the natural frequency of the drillstring to that of a drillstring in the field. Laboratory test apparatuses typically realize a higher natural frequency simply due to the significantly shorter length of the drillstring. By adding the flywheel to the drillstring, the rotational moment of inertia is increased, thus reducing the natural frequency. Figure 4.4 shows selected plotted results from a Rigid vs. Flywheel configuration comparison, including ROP vs WOB at 80 RPM, ROP vs WOB at 160 RPM, and torque vs ROP at 80 RPM. These plot formats were selected as they contain all significant results from the entire set of testing. Apparent in Figure 4.4 (a) and Figure 4.4 (b), the addition of the flywheel and corresponding reduction of the natural frequency results in a higher WOB required to enter Phase II drilling, which is the range of efficient drilling. Although Figure 4.4 (c) and Figure 4.4 (f) show that the torque required to achieve a given ROP doesn’t change with the reduction in natural frequency. The 5-blade bit displays a less obvious delay of efficient drilling due to the overall decrease in ROP, which is more apparent in the 160 RPM results (Figure 4.4 (e)) compared to the 80 RPM test (Figure 4.4 (d)).

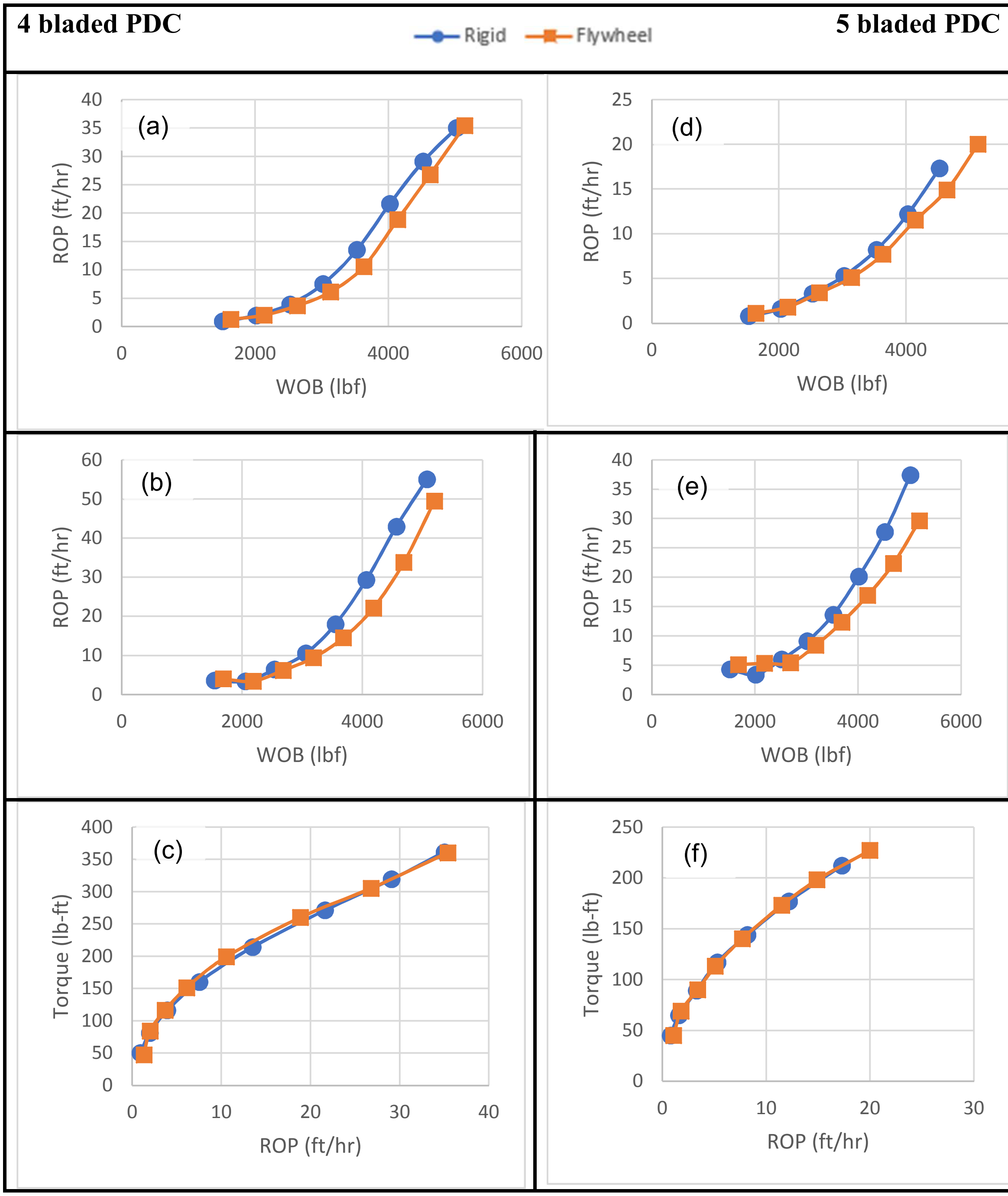


*Figure 4.4. Rigid vs Flywheel 4-Bladed 80RPM ROP vs WOB (a), 160RPM ROP vs WOB (b), 80RPM Torque vs ROP (c); 5-Bladed 80RPM ROP vs WOB (d), 160RPM ROP vs WOB (e), 80 RPM Torque vs ROP (f)*

## 4.3 Torsional Compliance Configuration

Torsional compliance testing was performed and analyzed for both the 4-blade and 5-blade bits. For these tests, the flywheel was removed because the use of the flywheel brought the torsional frequency below the targeted natural frequency designed for the tests. The torsional compliance is facilitated by two opposing torsional springs. The springs are preloaded to ensure non-zero torque while winding and unwinding during the drilling process. Table 4.3 shows the processed data for both the 4 and 5-blade PDC testing with torsional compliance.

*Table 4.3. Processed Torsional Compliance Data for the 4- & 5-Bladed PDC Bits*

| RPM | **4 Bladed PDC Bit** | | | | **5 Bladed PDC Bit** | | | |
|---|---|---|---|---|---|---|---|---|
| | WOB (lbf) | ROP (ft/hr) | Torque (lb-ft) | MSE (ksi) | WOB (lbf) | ROP (ft/hr) | Torque (lb-ft) | MSE (ksi) |
| 80 | 1485 | 1.1 | 41 | 190 | 1654 | 1.8 | 60 | 136 |
| | 1986 | 1.2 | 51 | 174 | 2071 | 1.4 | 72 | 192 |
| | 2428 | 1.9 | 76 | 129 | 2641 | 2.0 | 82 | 151 |
| | 2904 | 3.4 | 110 | 120 | 3145 | 3.6 | 103 | 101 |
| | 3385 | 5.2 | 137 | 92 | 3641 | 5.4 | 125 | 80 |
| | 3903 | 8.0 | 170 | 72 | 4101 | 7.9 | 150 | 64 |
| | 4397 | 13.2 | 217 | 53 | 4614 | 11.2 | 179 | 45 |
| | 4929 | 21.4 | 269 | 40 | 5184 | 15.9 | 212 | 42 |
| 120 | 1505 | 2.5 | 47 | 148 | 1587 | 3.7 | 69 | 114 |
| | 2037 | 2.1 | 62 | 166 | 2041 | 3.3 | 78 | 147 |
| | 2525 | 3.5 | 89 | 156 | 2544 | 3.2 | 80 | 152 |
| | 3036 | 5.8 | 115 | 112 | 3058 | 5.0 | 96 | 108 |
| | 3498 | 8.9 | 143 | 87 | 3546 | 7.5 | 116 | 84 |
| | 3999 | 14.2 | 183 | 66 | 4052 | 12.4 | 139 | 80 |
| | 4461 | 21.7 | 225 | 51 | 4561 | 13.2 | 164 | 49 |
| | 4962 | 32.4 | 274 | 38 | 5117 | 20.0 | 190 | 47 |
| 160 | 1486 | 5.3 | 72 | 122 | 1584 | 6.5 | 74 | 100 |
| | 1953 | 5.0 | 97 | 156 | 1988 | 7.0 | 92 | 107 |
| | 2468 | 4.3 | 92 | 178 | 2437 | 6.7 | 94 | 115 |
| | 2977 | 7.0 | 113 | 125 | 2992 | 7.2 | 100 | 111 |
| | 3445 | 10.4 | 138 | 98 | 3447 | 9.8 | 117 | 91 |
| | 3946 | 15.6 | 172 | 77 | 3965 | 14.5 | 139 | 69 |
| | 4419 | 22.2 | 202 | 62 | 4437 | 19.4 | 160 | 58 |
| | 4905 | 33.9 | 245 | 48 | 4963 | 27.1 | 191 | 49 |

Figure 4.5 shows the plotted data for the 4-bladed PDC and 5-bladed torsional compliance testing. Generally, for the 4-blade torsional compliance tests, there is approximately a 100 lbf in the applied

WOB compared to the rigid testing. Throughout all rotational speed tests, the torsional compliance configuration showed lower torque and ROP readings when compared to both the flywheel and rigid testing. However, all of the previously stated trends still hold with higher RPMs producing higher ROP values and lower torque values, especially at higher WOB. Unlike the 4-blade testing, the 5-blade testing typically shows a higher WOB relative to the step increments by about 100 lbf. Nearly all the previous trends and correlations are present in Figure 4.5 (d)-(f), although in Figure 4.5 (e), the 120 RPM test produces lower torque values at a given WOB than the 160 RPM, which does not follow the previous tests. Both the 120 and 160 RPM tests are lower than the 80 RPM tests except for the lowest WOB. Similar to the previous tests, the 5-bladed PDC produces lower ROP values, as well as lower torque compared to the 4-bladed PDC.

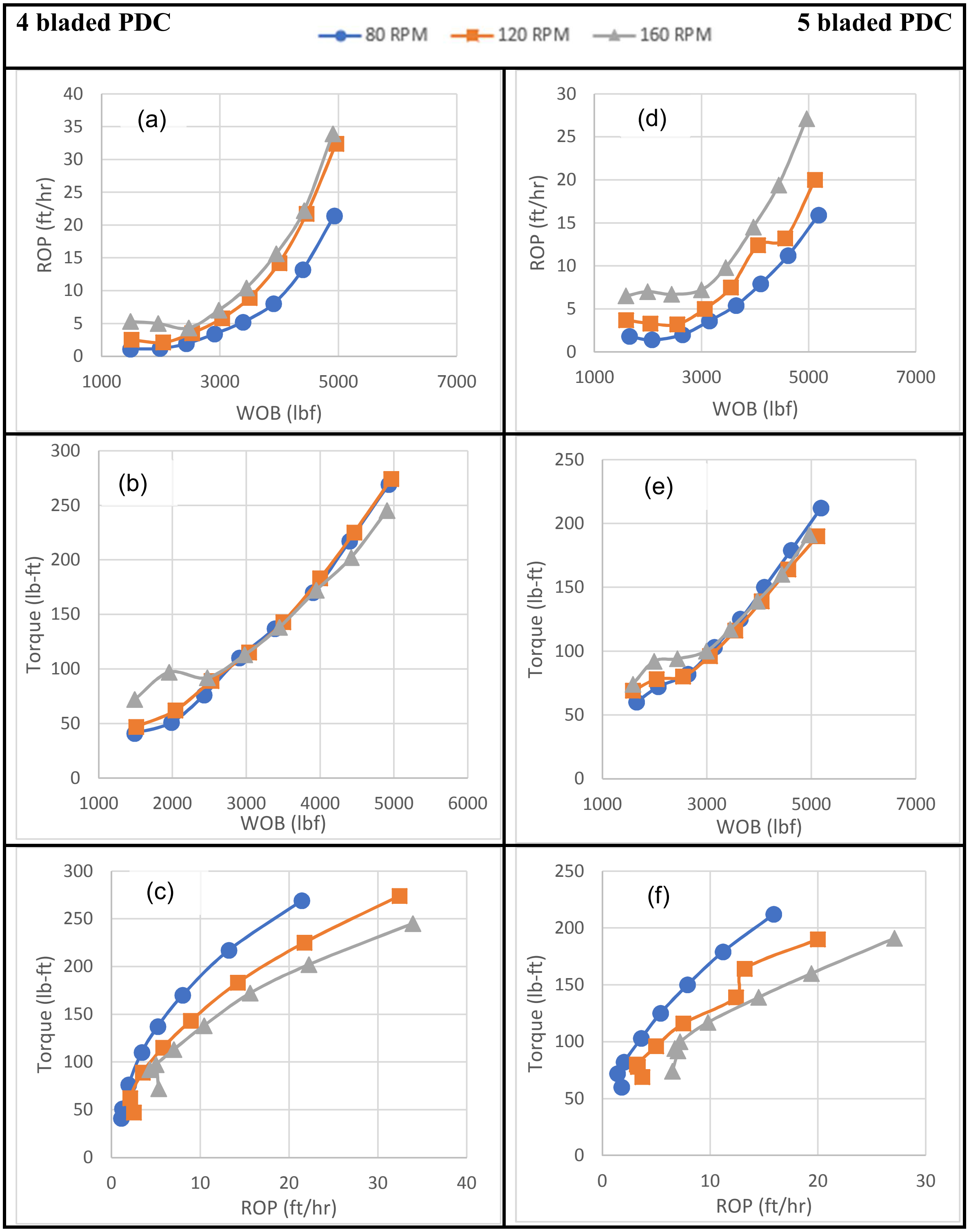


*Figure 4.5. ROP vs WOB (a), Torque vs WOB (b), Torque vs ROP (c) for 4-Bladed PDC; ROP vs WOB (d), Torque vs WOB (e), Torque vs ROP (f) for 5-Bladed PDC*

### 4.3.1 Rigid and torsional compliance configurations comparison

The torsional compliance configuration introduced a drillstring susceptible to torsional vibrations. Figure 4.6 shows a comparison of ROP vs WOB, and Torque vs ROP between the rigid baseline configuration and the torsional compliance configuration. The comparison below shows similar results to the rigid versus flywheel comparison, although to a more obvious extent. The introduction of the torsional compliance results in an increased WOB requirement to initiate Phase II drilling. This is apparent in both the 4- and 5-blade bits (Figure 4.6 (a), (b), (d), (e)). At 160 RPM, both configurations are operating in Phase I, or the inefficient drilling phase with low WOB. The torsional compliance configuration produces a slightly higher ROP, possibly due to the allowance of more effective bit-rock interaction, facilitated by the torsional suspension uptake. Similar to the rigid-flywheel comparison, the change in torque required to achieve a given ROP is negligible when torsional compliance is applied, as seen in Figure 4.6 (c) and Figure 4.6 (f).

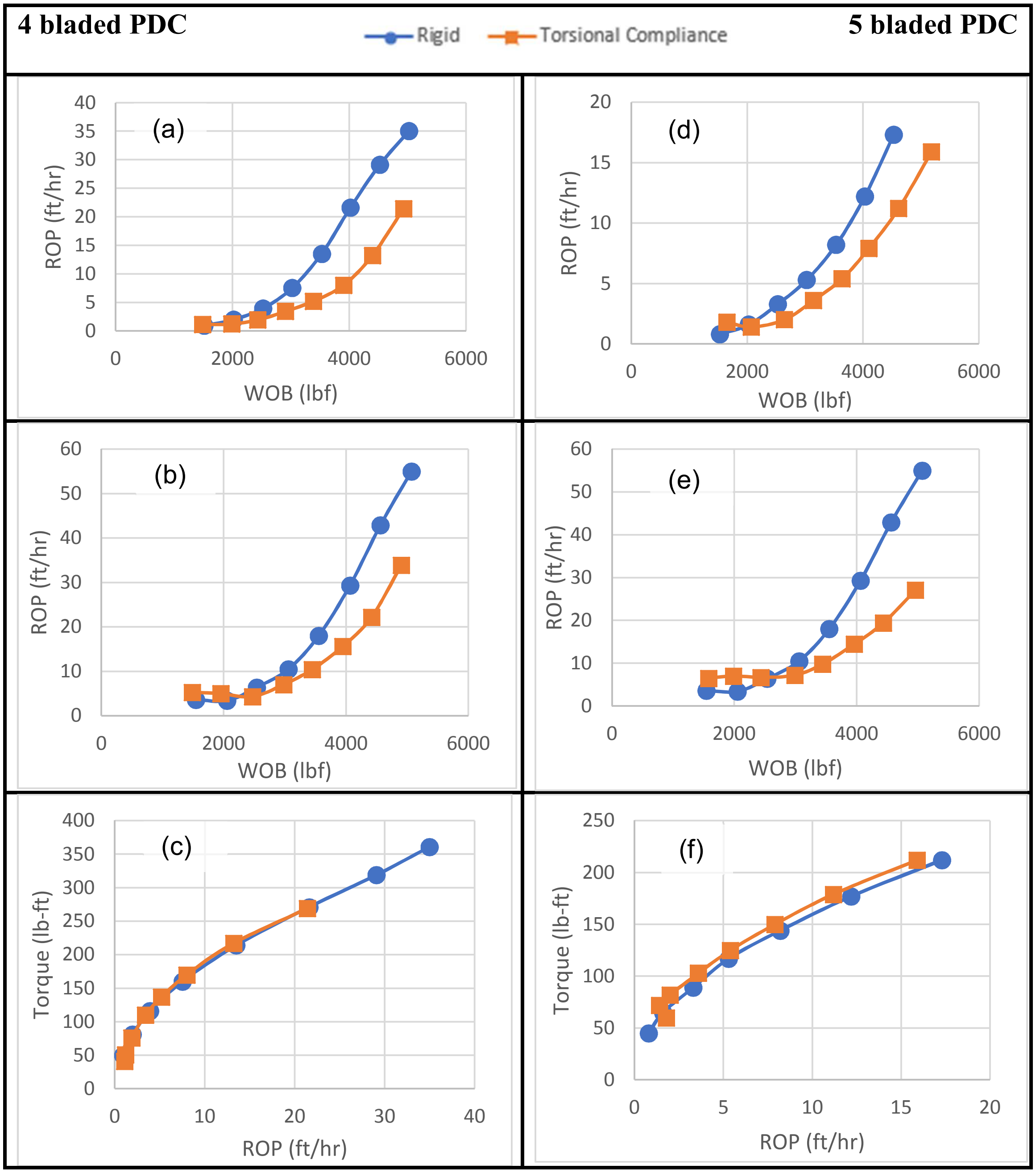


*Figure 4.6. Rigid vs Torsional Compliance 4-Bladed 80RPM ROP vs WOB (a), 160RPM ROP vs WOB (b), 80RPM Torque vs ROP (c); 5-Bladed 80RPM ROP vs WOB (d), 160RPM ROP vs WOB (e), 80 RPM Torque vs ROP (f)*

## 4.4 Wear Status Verification

The axial compliance and combined compliance tests were subsequently performed after the torsional compliance tests, and the final tests performed with the new bits were a retest of the rigid testing with an expectation that the results would be nearly identical to the initial rigid tests to ensure that bit wear wasn't a factor in the previous results. The format of the testing was dissimilar in that the drillstring wasn't reset to change RPM and the incremental applied WOB was less than initial rigid tests, i.e. WOB increments of approximately 1000 lbf compared to 500 lbf. Additionally, the tests were performed twice using computer controlled WOB and manually controlled WOB.

### 4.4.1 Computer controlled wob rigid verification tests

Table 4.4 shows the processed results for the rigid retests with computer controlled WOB. These tests have a similar relationship to one another in that the ROP increases as RPM increases as WOB increases. However, the ROP is noticeably lower than the original rigid tests, with the separation increasing as WOB increases, to a maximum of a roughly 65% decrease around 4500 lbs. Figure 4.7 shows the ROP vs. WOB plots for the 4- and 5-bladed retests, compared to the original rigid tests.

*Table 4.4. Processed Rigid Computer Controlled Verification Data for 4- & 5-Bladed PDC Bits*

| RPM | 4 Bladed PDC Bit | | | | 5 Bladed PDC Bit | | | |
|---|---|---|---|---|---|---|---|---|
| | WOB (lbf) | ROP (ft/hr) | Torque (lb-ft) | MSE (ksi) | WOB (lbf) | ROP (ft/hr) | Torque (lb-ft) | MSE (ksi) |
| 80 | 2302 | 1.1 | 48 | 120 | 2482 | 1.0 | 69 | 194 |
| | 3305 | 3.5 | 102 | 80 | 3476 | 2.8 | 102 | 100 |
| | 4308 | 7.5 | 150 | 55 | 4481 | 5.7 | 135 | 65 |
| | 4642 | 9.8 | 175 | 50 | 5479 | 10 | 181 | 50 |
| 120 | 2302 | 1.4 | 66 | 192 | 2479 | 1.8 | 86 | 199 |
| | 3305 | 4.9 | 102 | 86 | 3475 | 3.8 | 107 | 116 |
| | 4317 | 10.3 | 150 | 60 | 4480 | 7.9 | 140 | 73 |
| | 4596 | 12.4 | 168 | 56 | 5464 | 13.8 | 181 | 54 |
| 160 | 2293 | 2.6 | 79 | 167 | 2467 | 3.1 | 91 | 159 |
| | 3309 | 6.5 | 107 | 91 | 3476 | 4.7 | 111 | 130 |
| | 4305 | 13.8 | 157 | 62 | 4473 | 10 | 145 | 80 |
| | 4542 | 16.6 | 175 | 58 | 5434 | 17.2 | 179 | 57 |

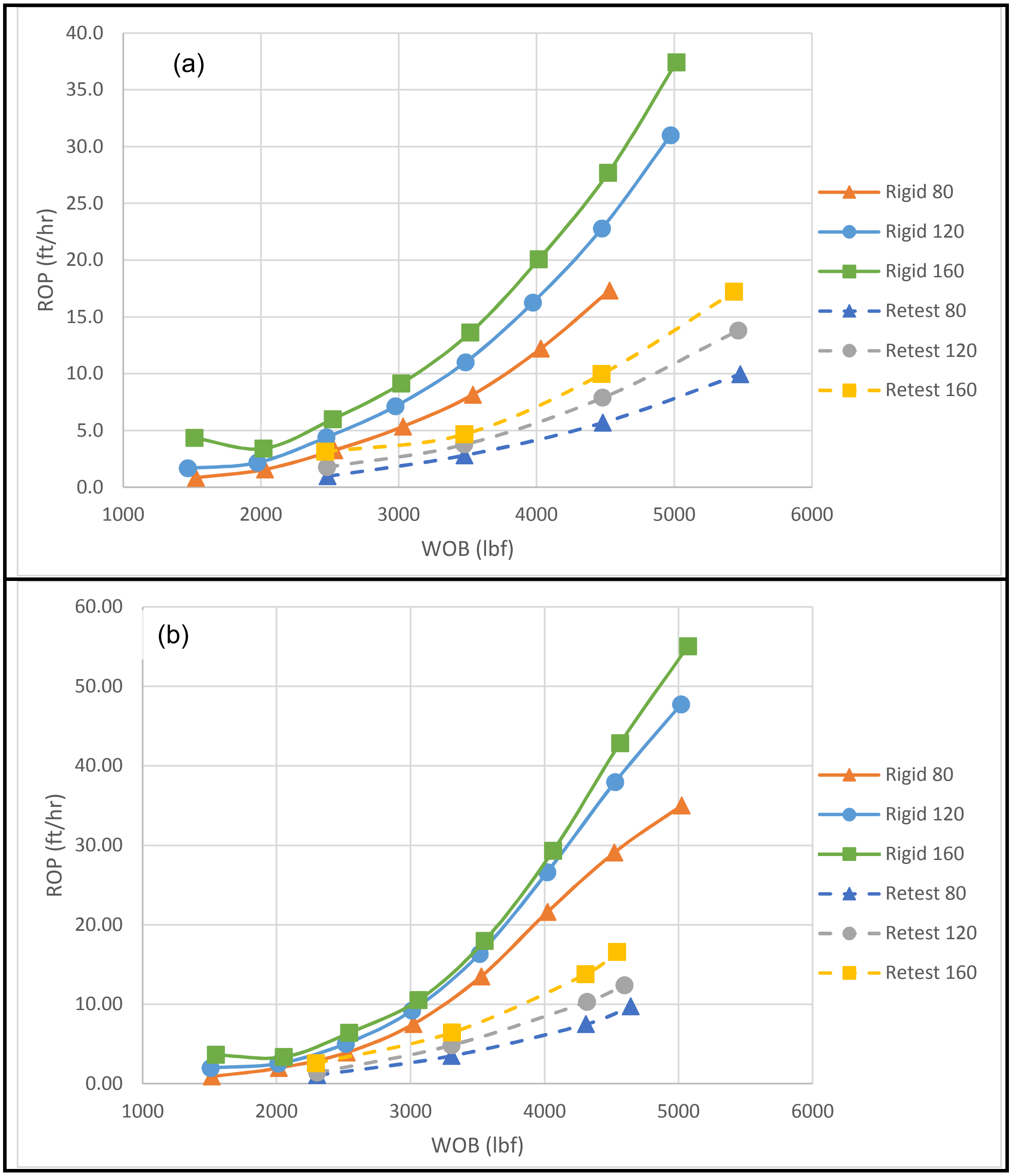


*Figure 4.7. Rigid Computer Controlled Verification (a) 4-Bladed ROP vs. WOB; (b)5-Bladed ROP vs. WOB*

### 4.4.2 Manually controlled wob rigid verification tests

Table 4.5 shows the processed results from the second, manually controlled WOB, rigid retests. These retests have an even smaller WOB range than the first retests. The maximum WOB is approximately 3400 lbs in both the 4- and 5-blade tests. While the ROP values don't differ much from computer controlled to manually controlled, the WOB range is too small to be able to distinguish whether confidently if the data would trend similarly. Due to this fact, the computer controlled WOB retest (verification #1) will be utilized for future comparisons. Figure 4.8 shows the ROP vs WOB plots for the 4- and 5-bladed retests compared to the original rigid tests.

*Table 4.5. Processed Manually Controlled Rigid Verification Data for 4- & 5-Bladed PDC Bits*

| RPM | **4 Bladed PDC Bit** | | | | **5 Bladed PDC Bit** | | | |
|---|---|---|---|---|---|---|---|---|
| | WOB (lbf) | ROP (ft/hr) | Torque (lb-ft) | MSE (ksi) | WOB (lbf) | ROP (ft/hr) | Torque (lb-ft) | MSE (ksi) |
| 80 | 1880 | 0.8 | 58 | 209 | 1918 | 0.9 | 58 | 171 |
| | 2248 | 1.0 | 72 | 197 | 2317 | 0.7 | 69 | 252 |
| | 2766 | 1.6 | 87 | 150 | 2853 | 1.3 | 85 | 181 |
| | 3385 | 3.2 | 125 | 108 | 3426 | 2.5 | 103 | 115 |
| 120 | 2027 | 0.7 | 74 | 429 | 1924 | 1.3 | 76 | 239 |
| | 2344 | 1.0 | 83 | 350 | 2296 | 1.5 | 79 | 213 |
| | 2756 | 2.0 | 97 | 203 | 2828 | 1.7 | 84 | 200 |
| | 3331 | 4.0 | 120 | 123 | 3379 | 3.2 | 101 | 130 |
| 160 | 1786 | 2.1 | 87 | 228 | 1820 | 2.8 | 85 | 168 |
| | 2160 | 2.7 | 96 | 195 | 2217 | 3.1 | 89 | 156 |
| | 2709 | 2.3 | 97 | 226 | 2751 | 4.0 | 99 | 136 |
| | 3292 | 4.7 | 119 | 139 | 3344 | 4.6 | 105 | 126 |

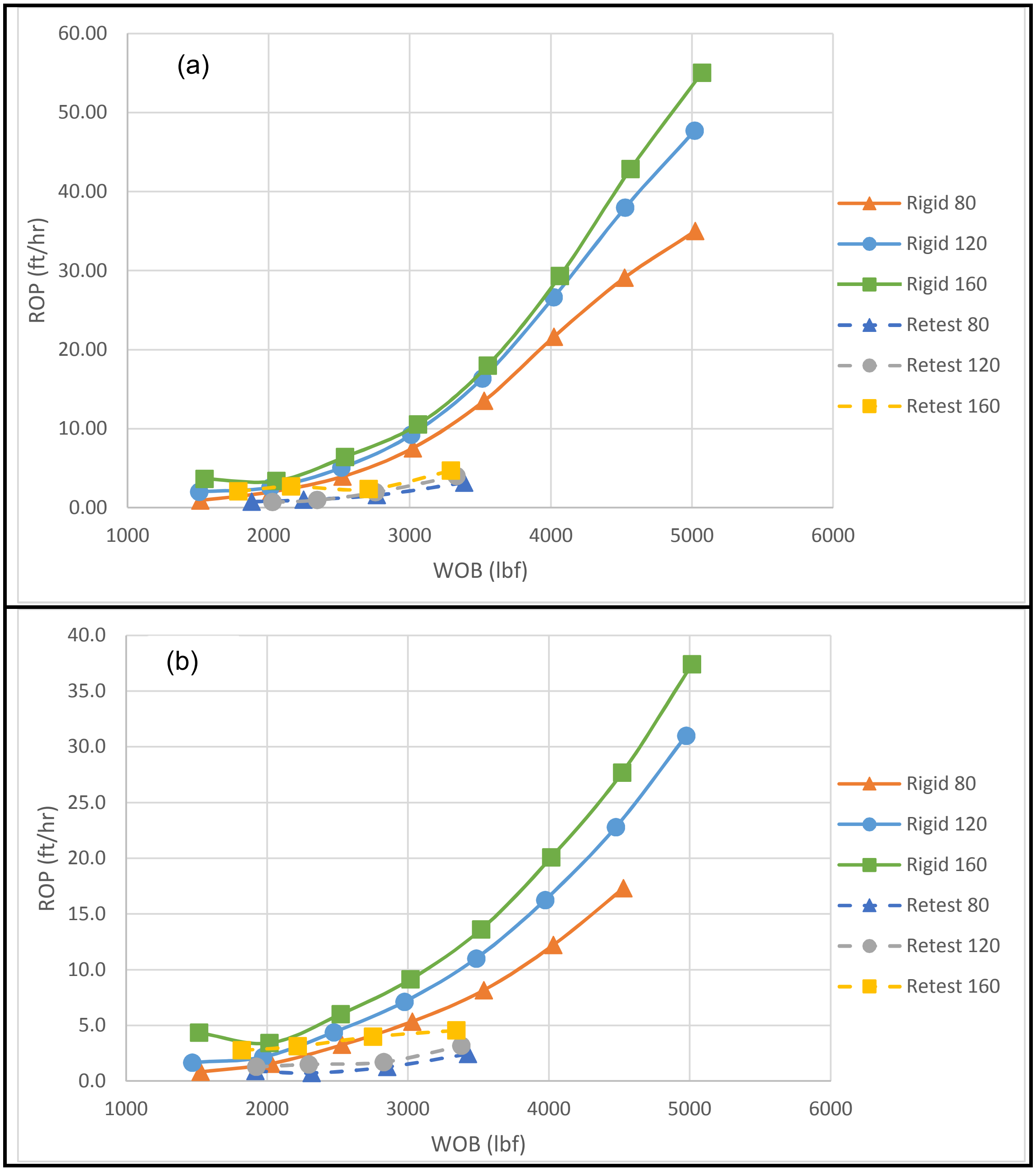


*Figure 4.8. Manually Controlled Rigid Verification (a)4-Bladed ROP vs. WOB; (b)5-Bladed ROP vs. WOB*

Upon evaluation, it was apparent that the rigid retest results were different than the original rigid configuration test results, namely the ROP values were significantly lower. Thus, the axial compliance and combined compliance comparisons will be performed with the rigid retest data.

## 4.5 Axial Compliance Configuration

The axial compliance testing didn't reach the same WOB ranges as the previous tests (rigid, flywheel, and torsional compliance). As such, bit performance couldn't be evaluated for this drillstring configuration above 3500 lbf. Table 4.6 shows the processed data for the axial compliance testing.

*Table 4.6. Processed Axial Compliance Data for 4- & 5-Bladed PDC Bits*

| RPM | **4 Bladed PDC Bit** | | | | **5 Bladed PDC Bit** | | | |
|---|---|---|---|---|---|---|---|---|
| | WOB (lbf) | ROP (ft/hr) | Torque (lb-ft) | MSE (ksi) | WOB (lbf) | ROP (ft/hr) | Torque (lb-ft) | MSE (ksi) |
| 80 | 1592 | 1.2 | 42 | 93 | 1687 | 0.7 | 45 | 174 |
| | 1688 | 0.8 | 40 | 137 | 1758 | 0.8 | 48 | 170 |
| | 1834 | 0.8 | 44 | 150 | 1968 | 1.0 | 54 | 141 |
| | 1939 | 0.9 | 56 | 180 | 2215 | 1.4 | 60 | 117 |
| | 2158 | 1.2 | 64 | 147 | 2422 | 1.8 | 68 | 102 |
| | 2276 | 1.5 | 69 | 127 | 2707 | 2.6 | 78 | 82 |
| | 2414 | 1.7 | 73 | 116 | 3010 | 3.9 | 89 | 63 |
| | - | - | - | - | 3356 | 4.5 | 102 | 63 |
| 120 | 1172 | 2.3 | 58 | 104 | 1310 | 2.5 | 48 | 77 |
| | 1389 | 2.9 | 82 | 115 | 1447 | 2.7 | 55 | 83 |
| | 1830 | 1.0 | 60 | 237 | 1769 | 3.1 | 66 | 87 |
| | 2082 | 1.4 | 62 | 182 | 2077 | 3.0 | 70 | 96 |
| | 2307 | 1.9 | 70 | 152 | 2375 | 3.0 | 73 | 100 |
| | 2620 | 2.8 | 82 | 118 | 2731 | 3.1 | 75 | 99 |
| | 2926 | 4.2 | 95 | 93 | 3062 | 5.6 | 84 | 61 |
| 160 | 1530 | 4.3 | 74 | 94 | 1573 | 7.4 | 55 | 41 |
| | 1780 | 4.2 | 79 | 103 | 1659 | 9.8 | 55 | 31 |
| | 2098 | 4.6 | 82 | 97 | 1862 | 9.0 | 62 | 38 |
| | 2376 | 3.5 | 81 | 128 | 2042 | 10.0 | 65 | 36 |
| | 2725 | 4.0 | 86 | 116 | 2300 | 10.0 | 69 | 38 |
| | 3008 | 6.5 | 98 | 82 | 2636 | 10.9 | 70 | 35 |
| | - | - | - | - | 2945 | 6.4 | 75 | 64 |

Figure 4.9 shows the same format of plots previously utilized, namely, ROP vs WOB at 80 RPM, ROP vs WOB at 160 RPM, and torque vs ROP at 80 RPM. At the lower WOB range of the testing, the axial results were not very different from those of the rigid testing, except for the 5-bladed tests at 120 RPM and 160 RPM, where the axial ROP values were higher than those of the rigid tests. It seems that the axial compliance results could track a similar pattern to that of the rigid results,

however, it’s impossible to confirm due to the WOB restriction, as well as the results at 120 RPM and higher are largely erratic and difficult to predict even within the available WOB range. The 5-bladed test at 80 RPM (Figure 4.9), shows the axial results following a similar path as the rigid, although reaching what appears to be a founder point at 3000 lbf. This contrasts with the 5-blade, 160 RPM test which shows elevated ROP values relative to the rigid results.

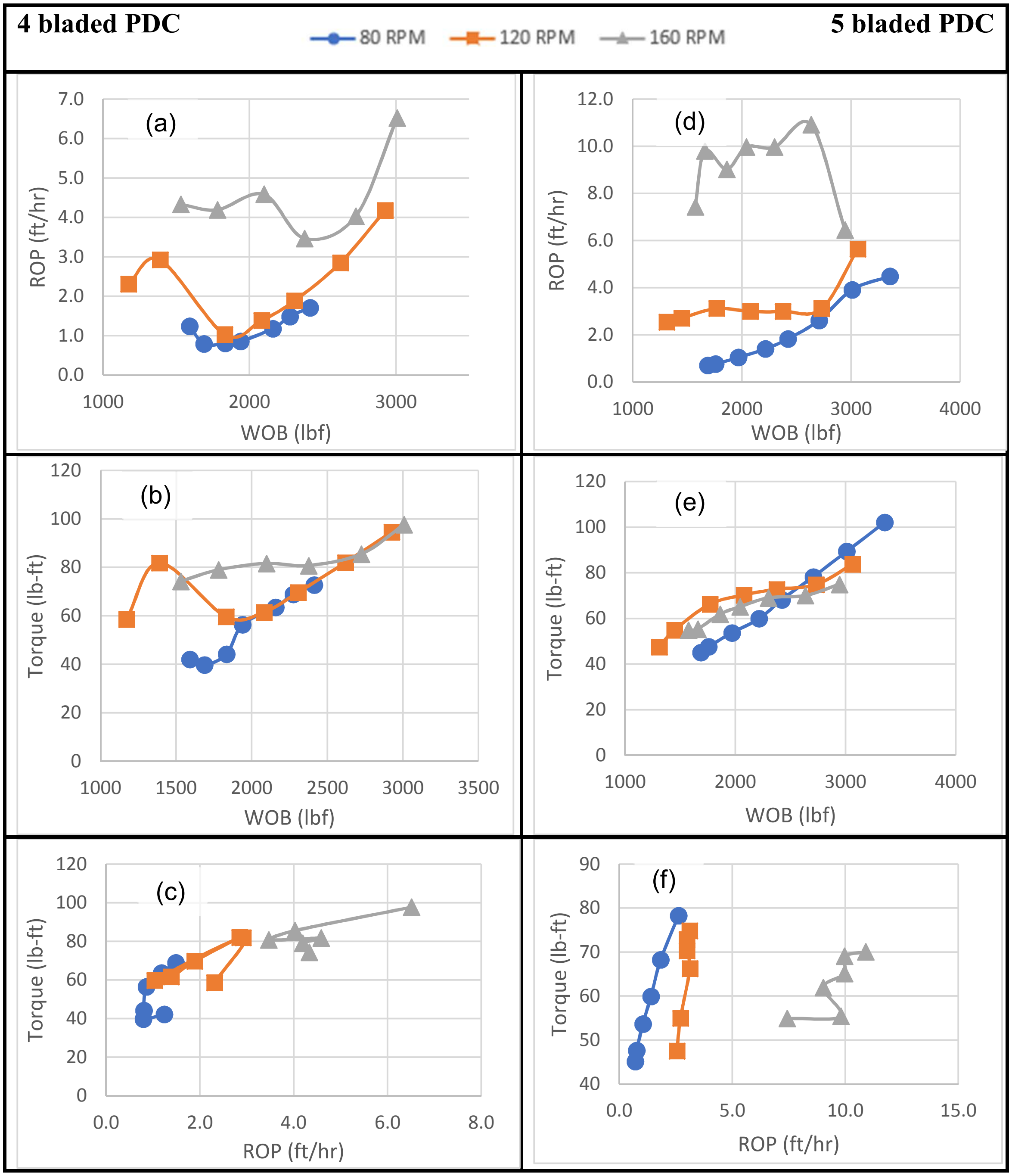


*Figure 4.9. ROP vs WOB (a), Torque vs WOB (b), Torque vs ROP (c) for 4-Bladed PDC; ROP vs WOB (d), Torque vs WOB (e), Torque vs ROP (f) for 5-Bladed PDC*

### 4.5.1 Rigid retest and axial compliance configurations comparison

As previously stated, the computer controlled verification test results are used instead of the original rigid baseline results due to discrepancies in the original data. Due to the restricted WOB range in the axial compliance data, accurate comparisons are difficult to draw in comparison to the rigid data. Figure 4.10 shows the comparison results for the rigid and axial compliance data. Figure 4.10 (a) and Figure 4.10 (d) show 80 RPM results for the 4 and 5-blade bits, and though the WOB values are low, it seems there is an indication that the axial compliance configuration reaches Phase II drilling at a lower WOB value than the rigid data. However, the 5-blade results show what seems to be a founder point, which would infer the axial compliance drillstring is subject to a much shorter WOB range in which efficient drilling can occur. In both 160 RPM comparisons (Figure 4.10 (b) and Figure 4.10 (e)), the axial results are too erratic to draw any conclusions from, especially in the case of the 5-blade bit. The 4-blade torque axial compliance trend (Figure 4.10 (c)), is also difficult to compare due to the restricted WOB and resultant ROP. Figure 4.10 (f) shows more definitive results, with the upper values of the axial compliance test having lower torque requirements for a given WOB value compared to the corresponding rigid test.

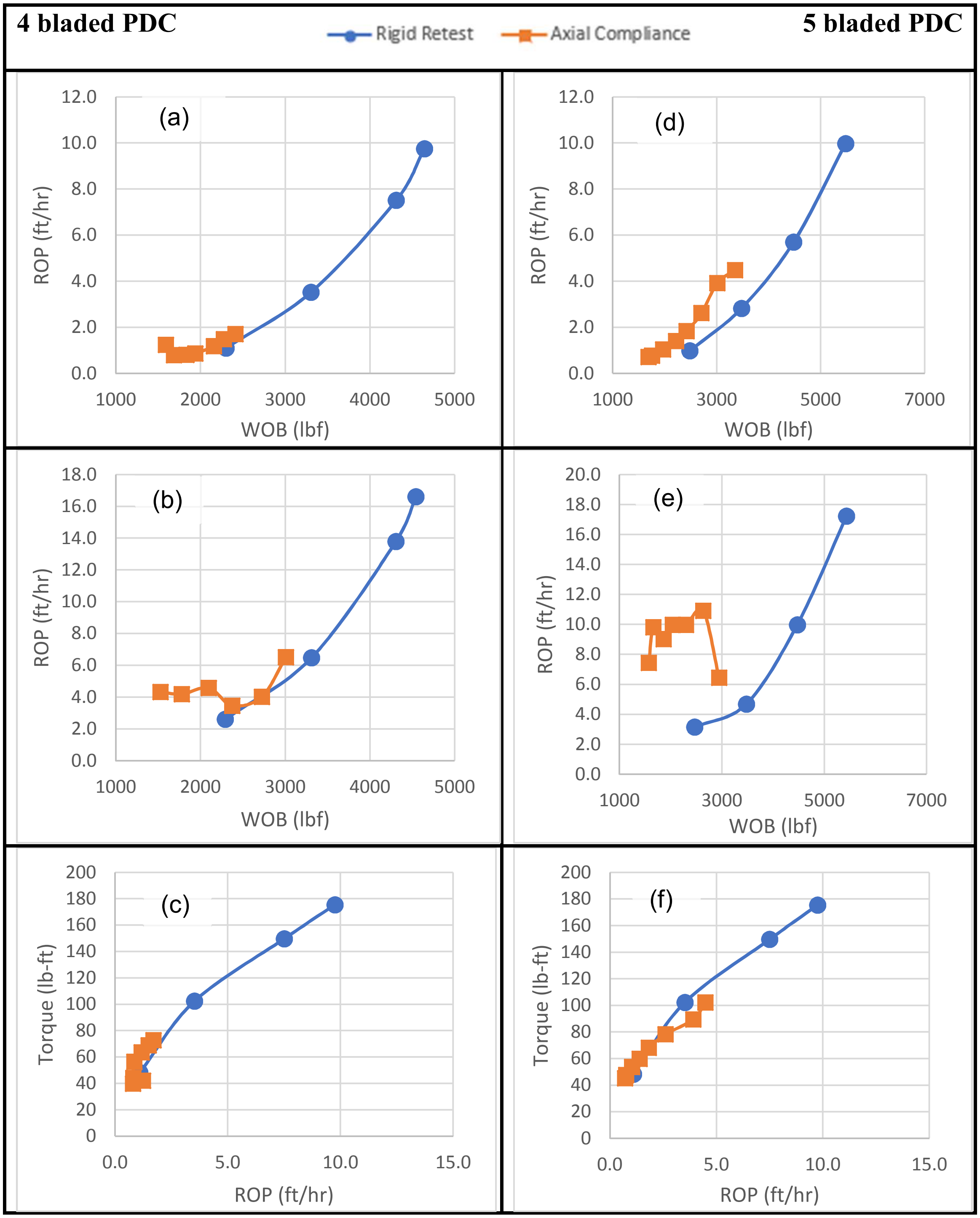


*Figure 4.10. Rigid vs Axial Compliance 4-Bladed 80RPM ROP vs WOB (a), 160RPM ROP vs WOB (b), 80RPM Torque vs ROP (c); 5-Bladed 80RPM ROP vs WOB (d), 160RPM ROP vs WOB (e), 80 RPM Torque vs ROP (f)*

## 4.6 Combined Torsional-Axial Compliance Configuration

Similar to the axial compliance tests, the combined compliance (torsional and axial compliance) tests have a reduced WOB range compared to the rigid, flywheel, and torsional compliance tests. Table 4.7 shows the processed data for the combined compliance data.

*Table 4.7. Processed Combined Compliance Data for 4- and 5-Bladed PDC Bits*

| RPM | **4 Bladed PDC Bit** | | | | **5 Bladed PDC Bit** | | | |
|---|---|---|---|---|---|---|---|---|
| | WOB (lbf) | ROP (ft/hr) | Torque (lb-ft) | MSE (ksi) | WOB (lbf) | ROP (ft/hr) | Torque (lb-ft) | MSE (ksi) |
| 80 | 1794 | 0.6 | 35 | 149 | 1643 | 1.3 | 73 | 74 |
| | 2068 | 0.8 | 40 | 143 | 1760 | 0.9 | 82 | 123 |
| | 2336 | 1.0 | 62 | 168 | 1986 | 1.0 | 86 | 127 |
| | 2552 | 1.4 | 72 | 136 | 2285 | 1.0 | 85 | 129 |
| | 2792 | 2.2 | 84 | 106 | 2535 | 1.3 | 90 | 111 |
| | 3060 | 4.0 | 95 | 65 | 2850 | 2.0 | 99 | 83 |
| | - | - | - | - | 3136 | 5.2 | 109 | 37 |
| 120 | 1366 | 2.5 | 41 | 67 | 1352 | 1.4 | 38 | 114 |
| | 1554 | 2.5 | 61 | 101 | 1558 | 1.8 | 46 | 107 |
| | 1876 | 2.2 | 72 | 134 | 1819 | 1.8 | 52 | 116 |
| | 2164 | 2.0 | 71 | 144 | 2128 | 1.7 | 53 | 127 |
| | 2456 | 1.9 | 71 | 149 | 2456 | 1.6 | 52 | 136 |
| | 2757 | 3.1 | 79 | 105 | 2730 | 2.2 | 59 | 111 |
| | 3072 | 4.4 | 92 | 86 | 3002 | 5.1 | 67 | 54 |
| 160 | 1371 | 3.5 | 63 | 98 | 1434 | 2.3 | 75 | 111 |
| | 1559 | 4.0 | 72 | 97 | 1533 | 2.7 | 79 | 101 |
| | 1794 | 4.0 | 75 | 104 | 1691 | 3.0 | 84 | 100 |
| | 2089 | 3.8 | 79 | 112 | 2021 | 3.3 | 89 | 99 |
| | 2398 | 3.4 | 77 | 123 | 2341 | 3.4 | 92 | 101 |
| | 2738 | 3.5 | 79 | 124 | 2719 | 2.8 | 89 | 119 |
| | 3016 | 6.6 | 91 | 75 | 3012 | 4.9 | 97 | 75 |

Figure 4.11 shows the plotted combined compliance data. The combined data results in lower ROP values of the same magnitude, and trends most similarly to the axial compliance tests, implying the axial vibrations are much more influential to overall bit performance than the torsional vibrations. While overall, the tests (aside from the magnitude of the ROP) follow relatively similar trends to

the other tests in most data comparisons, the torque versus ROP plots shows significant unpredictability in this WOB range, except in the 4-blade 80 RPM test.

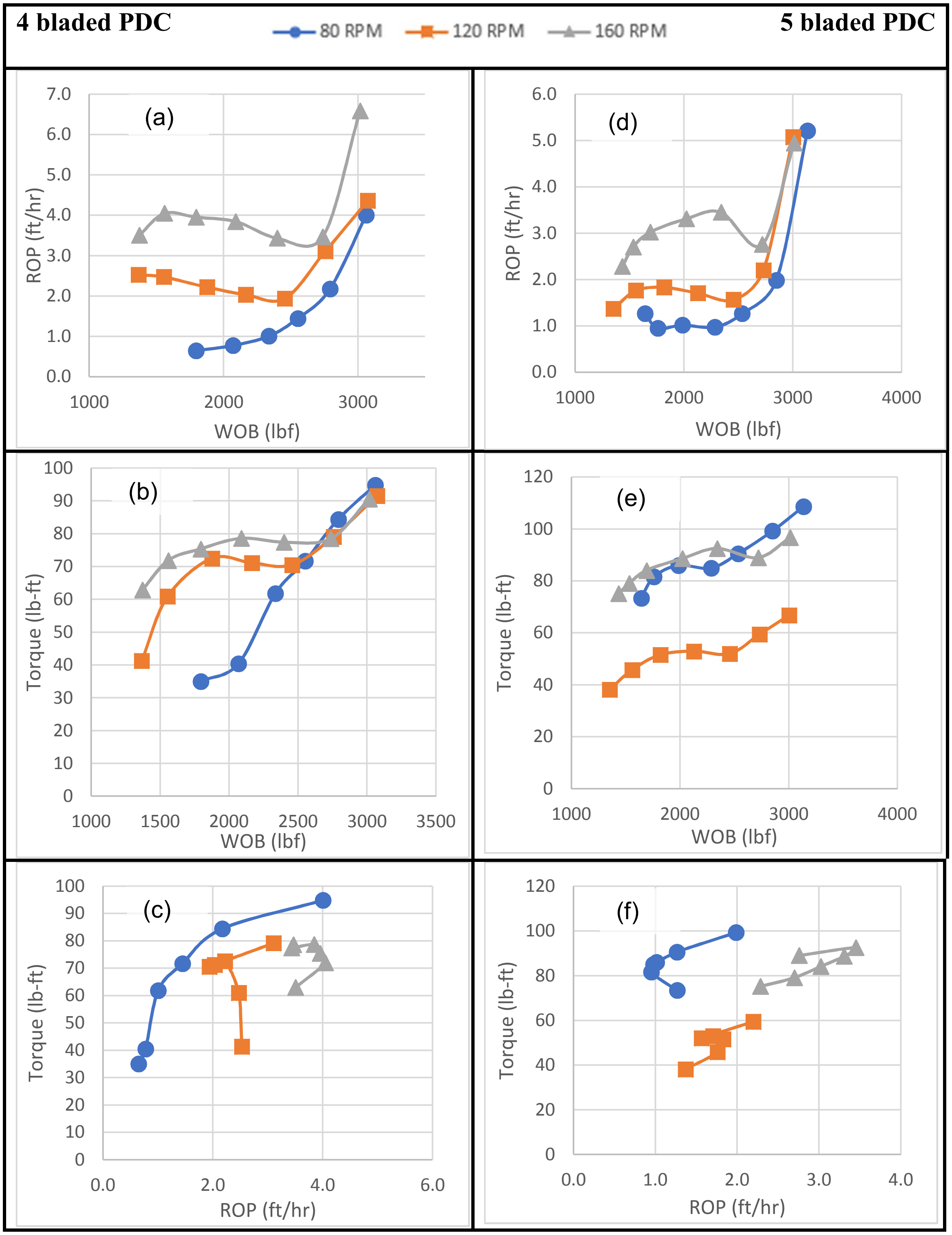


*Figure 4.11. ROP vs WOB (a), Torque vs WOB (b), Torque vs ROP (c) for 4-Bladed PDC; ROP vs WOB (d), Torque vs WOB (e), Torque vs ROP (f) for 5-Bladed PDC*

### 4.6.1 Rigid retest and combined torsional-axial compliance comparison

The combined compliance data is also subject to a reduced WOB range, and as seen in Figure 4.11, the results can become quite erratic at increased RPM values, which shows that the axial component of the compliance is prevalent in this configuration. Figure 4.12 (a) and Figure 4.12 (d) show the 80 RPM ROP vs. WOB plots, which in both cases show similar relationships at low WOB values, but with an apparent encroachment into Phase II drilling between the last two data points. While the axial compliance comparisons showed a drastically shortened Phase II period, the torsional compliance component in this combined case appears to counter that shortening. As thus, there could be a clear Phase II trend if higher WOB data points were available. Figure 4.12 (b) and Figure 4.12 (e) show very similar results for the 160 RPM tests, though a more definitive collection of relatively increased ROP in Phase I drilling region. Both torque plots (Figure 4.12 (c) and Figure 4.12 (f)) show trends of a rapidly increasing torque requirement to achieve ROP at the lowest WOB values, though that requirement quickly begins to plateau, and the required torque to achieve a given ROP becomes less than that of the rigid configuration.

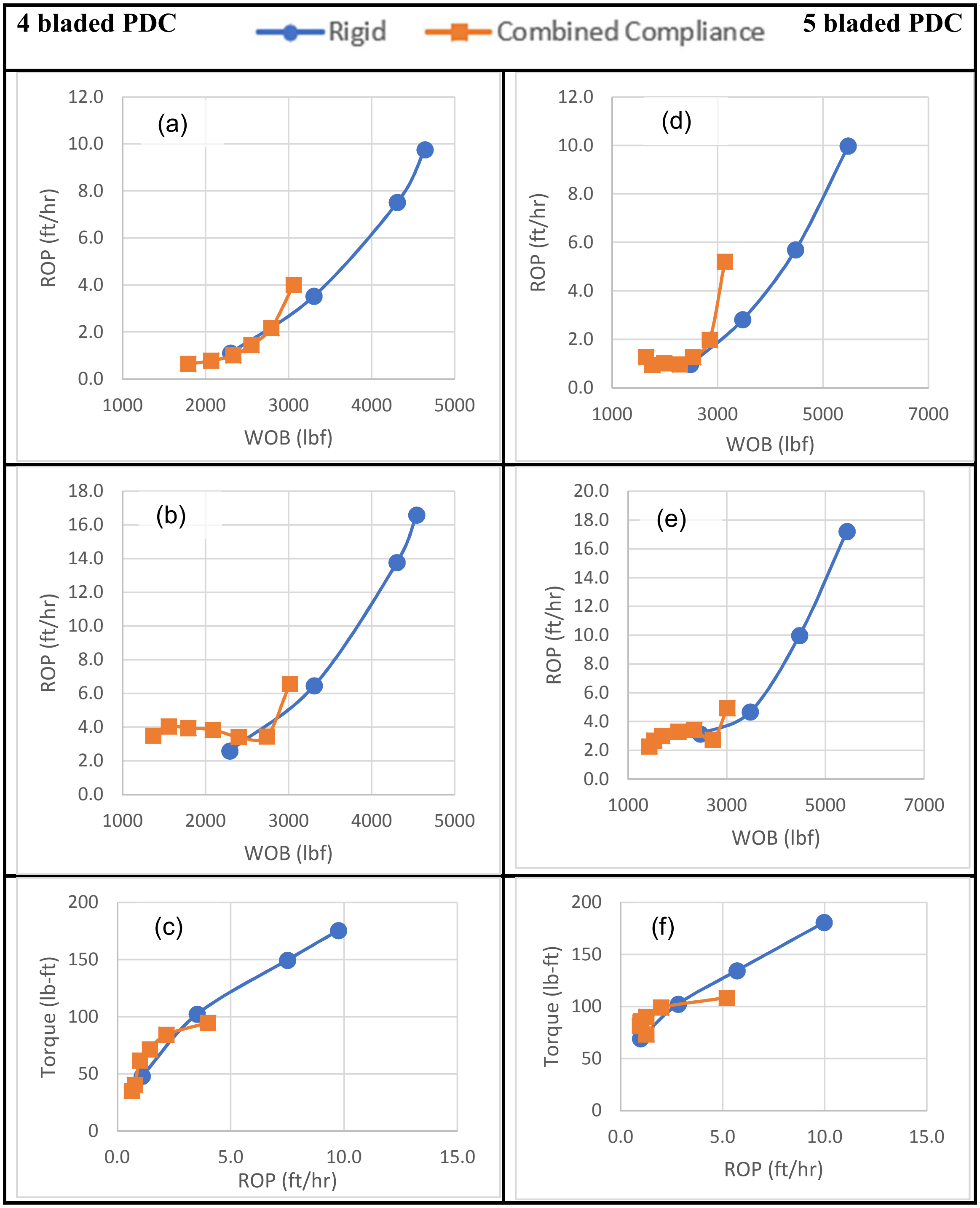


*Figure 4.12. Rigid vs Combined Compliance 4-Bladed 80RPM ROP vs WOB (a), 160RPM ROP vs WOB (b), 80RPM Torque vs ROP (c); 5-Bladed 80RPM ROP vs WOB (d), 160RPM ROP vs WOB (e), 80 RPM Torque vs ROP (f)*

## 4.7 Worn Bit Evaluation

After all new bit testing was completed, the bits were artificially worn for the purpose of evaluating the effect of bit wear on drilling performance. Similar to the axial and combined compliance testing, the worn data is compared to the computer controlled retest dataset. Table 4.8 shows the processed results for the rigid worn bit data. Figure 4.13 provides an image of one of the PDC bits after it has been artificially worn.

*Figure 4.13. Artificially Worn PDC Bit*

*Table 4.8. Processed Rigid Worn Data for 4- & 5-Bladed PDC Bits*

| RPM | 4 Bladed PDC Bit | | | | 5 Bladed PDC Bit | | | |
|---|---|---|---|---|---|---|---|---|
| | WOB (lbf) | ROP (ft/hr) | Torque (lb-ft) | MSE (ksi) | WOB (lbf) | ROP (ft/hr) | Torque (lb-ft) | MSE (ksi) |
| 80 | 1821 | 0.2 | 16 | 212 | 1744 | 0.2 | 12 | 200 |
| | 2333 | 0.3 | 21 | 200 | 2246 | 0.2 | 18 | 250 |
| | 2830 | 0.4 | 33 | 205 | 2739 | 0.5 | 29 | 157 |
| | 3333 | 0.6 | 48 | 207 | 3238 | 0.6 | 39 | 174 |
| | 3821 | 0.8 | 64 | 219 | 3745 | 1.1 | 59 | 153 |
| | 4326 | 1.0 | 77 | 222 | 4242 | 0.9 | 76 | 222 |
| | 4826 | 1.2 | 94 | 209 | 4733 | 1.1 | 87 | 218 |
| | 5333 | 1.4 | 129 | 257 | 5239 | 1.3 | 94 | 198 |
| 120 | 1804 | 0.1 | 18 | 702 | 1770 | 0.2 | 12 | 204 |
| | 2307 | 0.2 | 29 | 525 | 2267 | 0.4 | 22 | 232 |
| | 2805 | 0.1 | 35 | 997 | 2773 | 0.7 | 37 | 230 |
| | 3299 | 0.8 | 69 | 355 | 3300 | 1.0 | 59 | 231 |
| | 3803 | 1.2 | 100 | 353 | 3773 | 1.8 | 78 | 177 |
| | 4301 | 1.3 | 134 | 435 | 4270 | 2.3 | 86 | 157 |
| | 4799 | 1.7 | 158 | 385 | 4782 | 2.6 | 98 | 155 |
| | 5301 | 2.0 | 169 | 343 | 5255 | 2.9 | 108 | 151 |
| 160 | 1831 | 0.1 | 20 | 754 | 1815 | 0.3 | 6 | 107 |
| | 2339 | 0.2 | 27 | 634 | 2318 | 0.4 | 14 | 175 |
| | 2834 | 0.3 | 33 | 632 | 2818 | 0.7 | 25 | 201 |
| | 3336 | 1.2 | 71 | 315 | 3325 | 0.9 | 40 | 237 |
| | 3841 | 1.3 | 101 | 431 | 33820 | 1.5 | 59 | 213 |
| | 4340 | 1.7 | 129 | 411 | 4320 | 2.9 | 78 | 150 |
| | 4839 | 2.4 | 146 | 333 | 4821 | 3.7 | 91 | 134 |
| | 5340 | 2.9 | 158 | 298 | 5315 | 4.5 | 102 | 123 |

The worn tests resulted in substantially lower ROP values, especially as WOB is increased. At the lowest common WOB values (approximately 2300 lbs), the results show a decrease of approximately 1 ft/hr, which is significant due to the rigid results having ROP values of around only 1 ft/hr. Thus, the worn ROP values are barely above 0 until roughly 3500 lbs WOB is reached. The maximum difference at common WOB values of approximately 4600 lbs WOB is a nearly 90% decrease in performance. Additionally, the torque values in the new bit tests are significantly higher than the worn bit torque values, implying the bit wear significantly decreases the ability of the bit to engage with the hard rock. Figure 4.14 shows the ROP vs WOB worn-rigid plots for the 4- and 5-bladed tests.

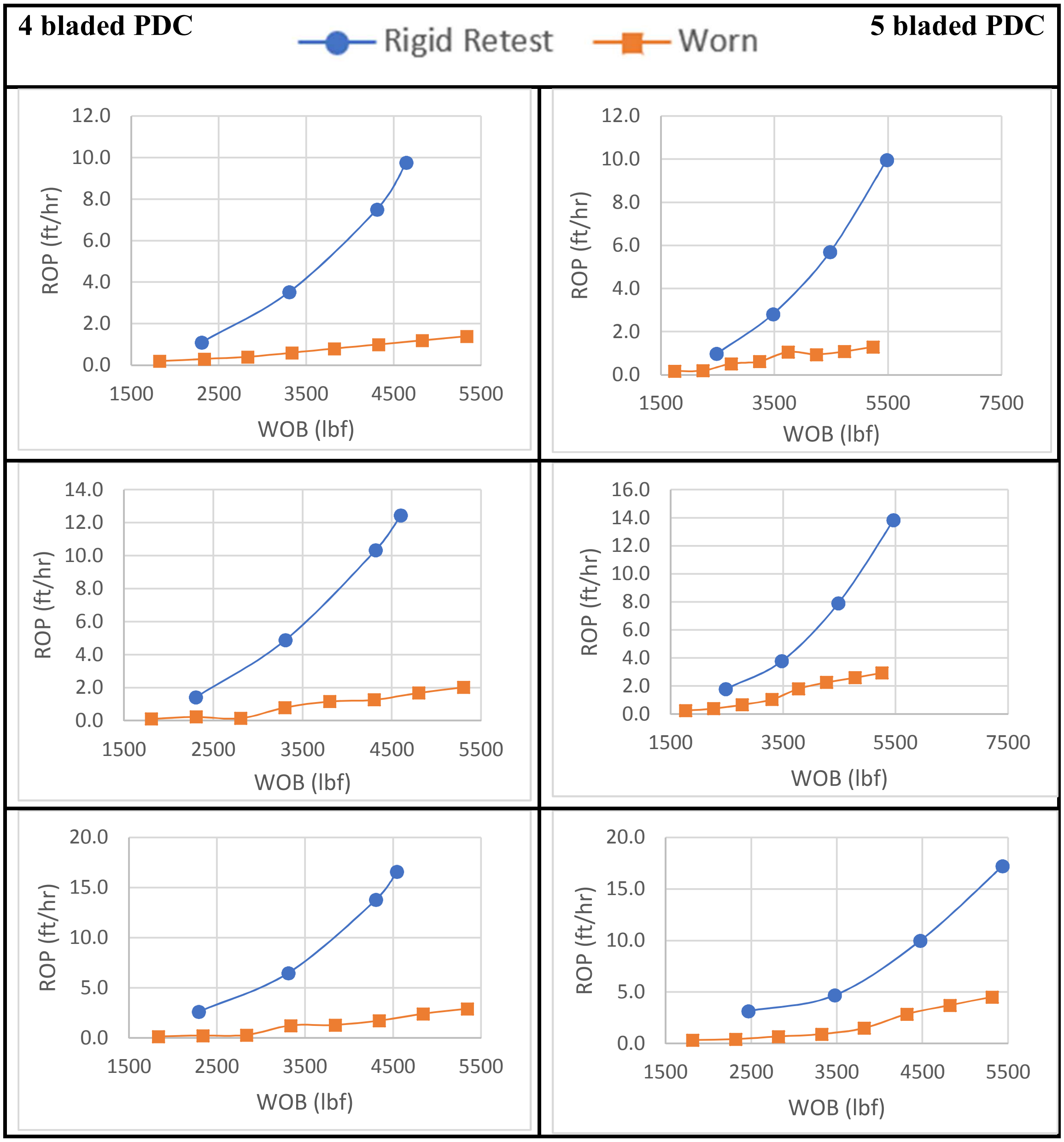


*Figure 4.14. ROP vs WOB 80 RPM(a), 120 RPM (b), 160 RPM (c) for 4-Bladed PDC; 80 RPM (d), 120 RPM (e), 160 RPM (f) for 5-Bladed PDC*

CHAPTER V

# 5 DISCUSSION

## 5.1 Rigid Configuration Test Data

The objective of the rigid retest was to verify the wear status of the bit after performing several drilling tests. Thus, the test data of the rigid and retest were expected to be similar since the bits were expected to have no wear after testing. However, the rigid retest results were much lower than the original rigid testing as seen in Figure 4.7 and Figure 4.8.

The computer controlled and manually controlled rigid retests results were approximately in the same range, except for the fact that the manually controlled retest did not evaluate the full range of WOB values. The computer controlled test, retest #1, begins at approximately 2300-2400 lb WOB for both bits, progresses up to 4600 lb WOB for the 4-blade PDC, and up to 5500 lb for the 5-blade PDC. This is a sufficient range to compare with the compliance tests performed. However, the manually controlled test, retest #2, begins at 1800-2000 lb for both bits. The subsequent data points, falling between 2200 and 2400 lb for both bits, seem to agree with the computer controlled test in terms of ROP results. Although the testing ends for both bits at a maximum of 3400 lb. While all data points provided from the manually controlled test match the ROP results produced by the computer controlled test, the maximum WOB reached is not sufficient for comparison to the compliance tests, and for that reason, the computer controlled retest was utilized for the comparison with different drillstring configurations.

Initially, it was suspected that the WOB indicator could have been off since several transducers had failed throughout the testing. As such, an attempt to recalibrate the WOB by shifting the measured WOB to match the original rigid test ROP. Figure 5.1 shows a comparison of the rigid and re-calibrated rigid-retest with an offset of 750 lbs for the 4-bladed bit at 80 and 160 RPM.

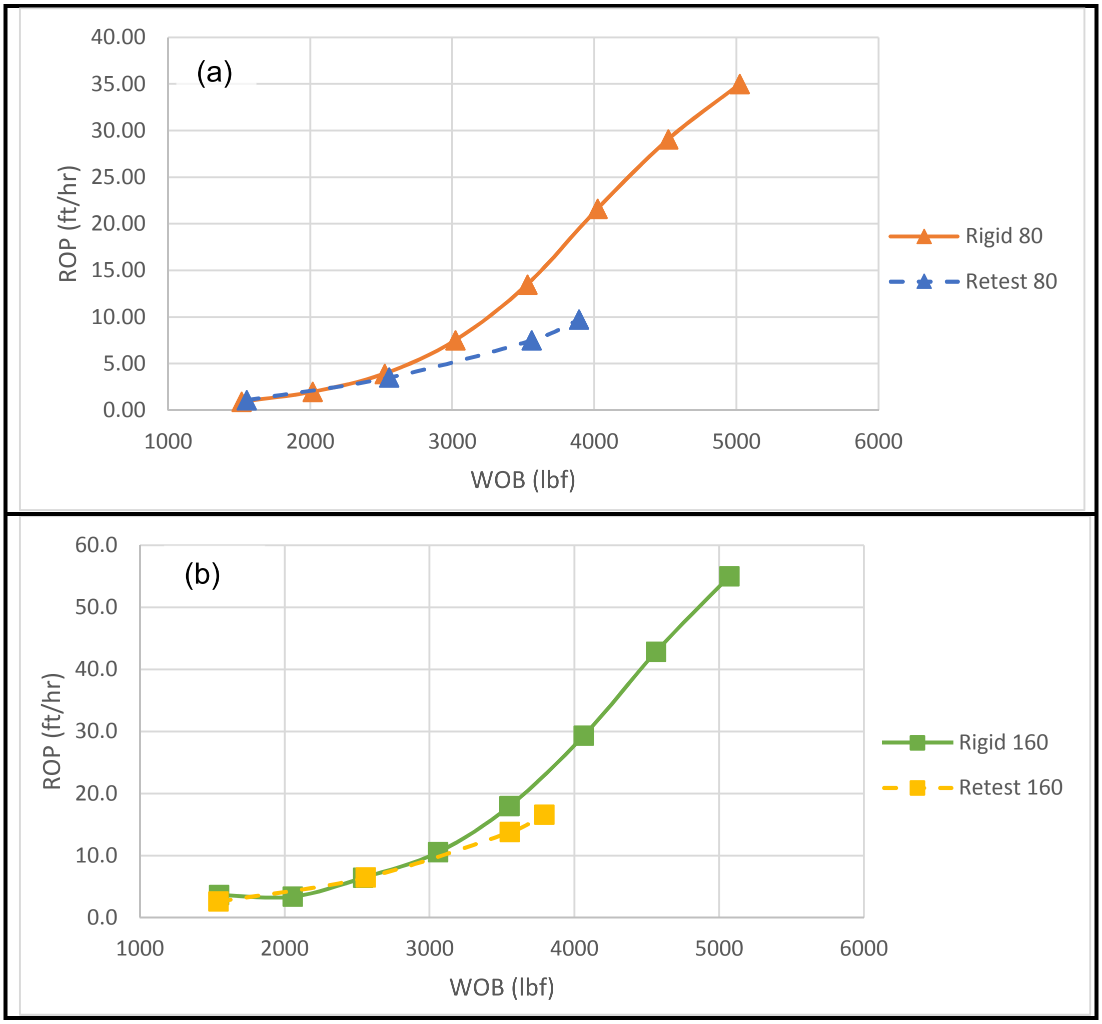


*Figure 5.1. Rigid vs Computer Controlled Retest for 4-Blade (a) 80RPM and (b) 160 RPM*

It can be seen in Figure 5.1 that the recalibrated retest results match well with the lower range of the original rigid baseline ROP, however, as WOB increases where the original rigid test behaves linearly in phase II efficient drilling, the calibrated retest deviated from the original data. The behavior seen with the re-test data shows that the efficient drilling phase was not reached during the testing. Based on this analysis, it was decided that the reason for the deviation between the rigid and retest is not due to the WOB measurement indicator and more testing is required to measure the repeatability of the results.

## 5.2 Effect Of Test Configuration On Rop

### 5.2.1 Rigid baseline, flywheel, and torsional compliance configurations

The original rigid baseline, flywheel, and torsional compliance testing were all performed in a single period of testing, and thus although it has been determined that the original rigid baseline performance results are inflated, the relationship between the configurations is still the same, so quality comparisons can still be made. The axial compliance and combined axial-torsional compliance tests were compared with the computer controlled rigid retest performance results.

To show a clear comparison of the ROP behavior for the first three configurations, three WOB levels were selected for each rotational speed test. Linear interpolation was used to calculate the ROP of each test configuration at their respective applied rotational speed for the selected three WOB levels. The selected WOB levels represent a low range at 1700 lb, an intermediate range at 3050 lb, and a high range at 4850 lb. Figure 5.2. shows the calculated ROP, using linear interpolation, comparison for the 4-blade rigid, flywheel, and torsional compliance configurations for all applied rotational speeds.

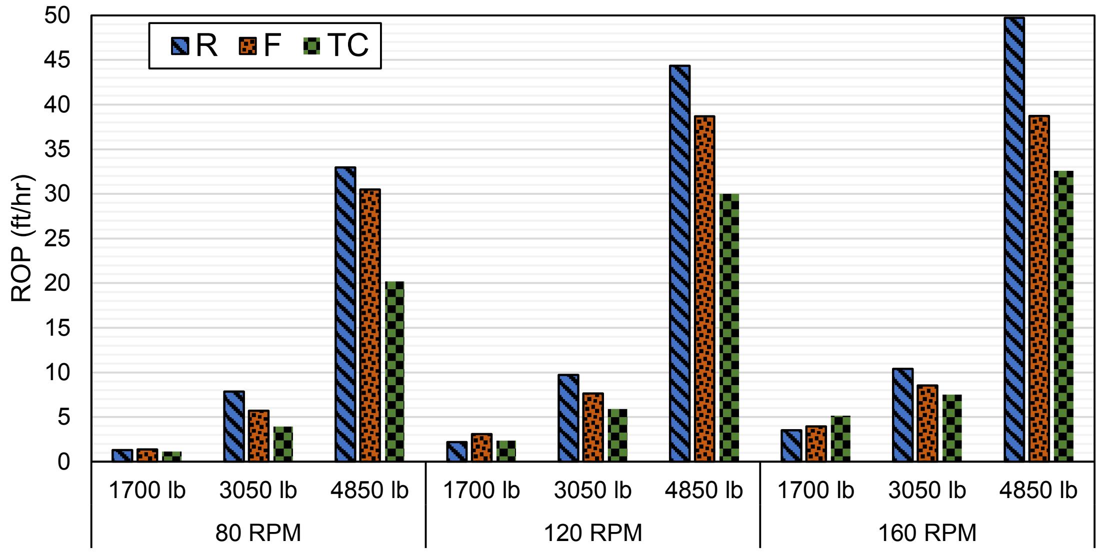


*Figure 5.2. ROP Comparison of Rigid (R), Flywheel (F), and Torsional Compliance (TC) Configurations with the 4-Bladed PDC*

At a WOB of 1700 lb, the flywheel and torsional compliance generally showed higher ROP for all applied rotational speeds except for the torsional compliance at 80 RPM, which showed a 13% decrease compared to the rigid configuration. For the intermediate and high WOB levels, the rigid test configuration showed consistently higher ROP compared to the torsionally compliant and flywheel configurations (Figure 5.2.). For instance, at 3050 lb WOB, the flywheel configuration showed an ROP decrease of 27%, 22%, and 18% at 80, 120, and 160 RPM, respectively, compared to the rigid with an average decrease of 22% for all rotational speeds. Similar behavior for the torsional configuration at 3050 lb WOB can be noticed with a 50%, 40%, and 28% decrease compared to rigid at 80, 120, and 160 RPM with an average decrease of 39%. At a high WOB of 4850 lb, the flywheel configuration showed an ROP decrease of 7%, 13%, and 22% at 80, 120, and 160 RPM compared to rigid with an average decrease of 14% while the torsional compliance configuration showed 39%, 32%, and 34% at 80, 120, and 160 RPM with an average decrease of 35%.

The same procedure was applied to the 5-blade bit, where the only difference is that the high range of WOB is at 4500 lb compared to the 4-blade bit. The comparison of the calculated ROP, using linear interpolation, for the 5-blade bit at three WOB intervals is shown in Figure 5.3. Similar behavior to the 4-blade bit at low WOB, i.e. WOB of 1700 lb, can be noticed with the flywheel and torsional compliance configurations showing higher ROP than the rigid. At the intermediate and high WOB levels, the rigid configuration shows higher ROP compared to the flywheel and torsional compliance at all rotational speeds, where an average decrease of 19% and 33% in ROP can be seen for the flywheel and torsional compliance, respectively, for all rotational speeds.

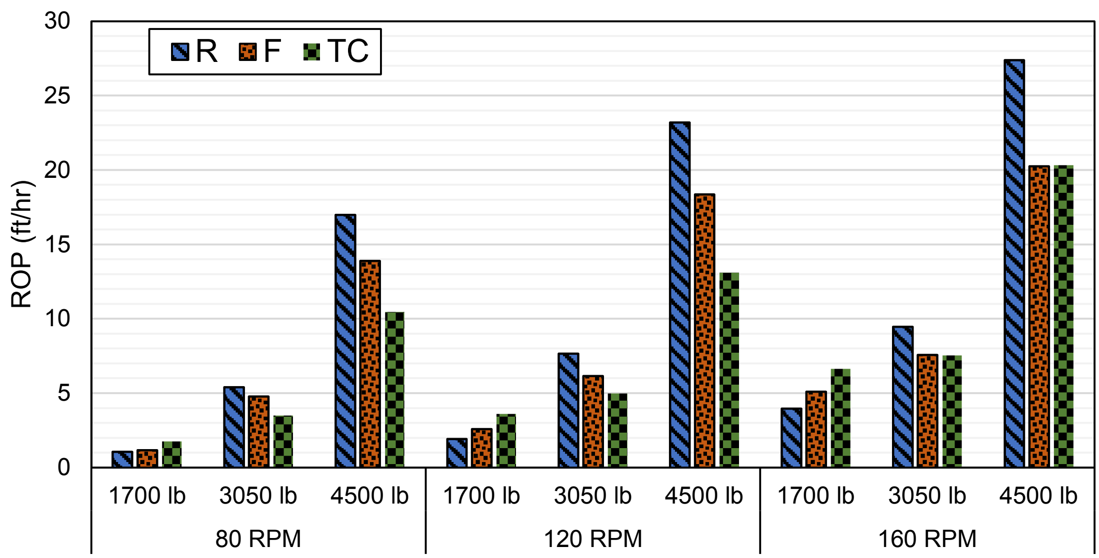


*Figure 5.3. ROP Comparison of Rigid (R), Flywheel (F), and Torsional Compliance (TC) Configurations with the 5-Bladed PDC*

At a set of rotational speeds, the torque generated with PDC bits can be used to analyze the drilling performance of a drill bit. Figure 5.4. shows the torque versus ROP for the 4-bladed bit at 80 RPM for the three drilling configurations. A linear line is fitted for each test configuration as seen in Figure 5.4., which describes the amount of torque required to produce a given ROP based on the test configuration. The higher the slope of the line fit the more torque is required to achieve a certain ROP. The line fit of the rigid and flywheel test configurations shows a similar slope at 80 RPM, indicating that the flywheel setup has no significant effect on the transmitted torque to the bit. However, the torsional compliance test, which mimics the drillstring torsional vibrations, shows a higher slope indicating higher torque is required to reach the same ROP as the rigid and the flywheel configurations.

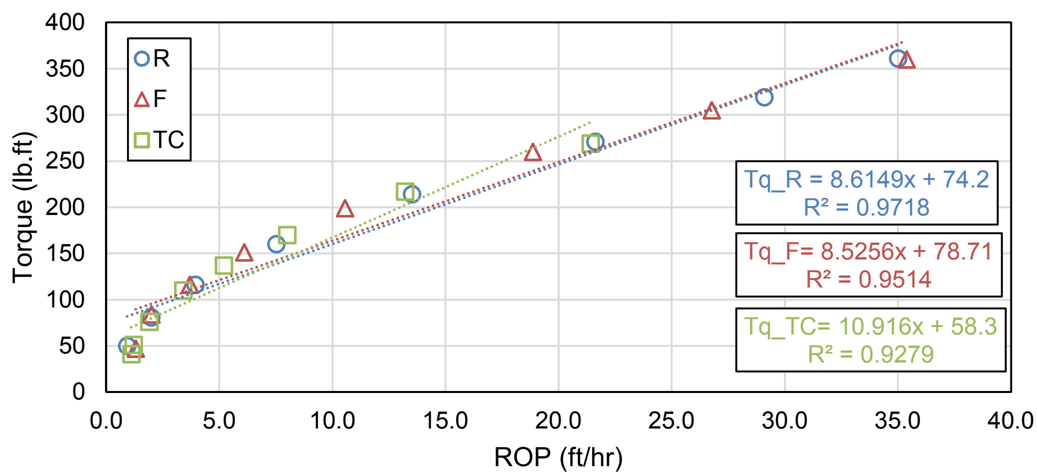


*Figure 5.4. Torque vs. ROP at 80 RPM for the 4-bladed PDC Bit with Rigid (R), Flywheel (F), and Torsional Compliance (TC) Configurations*

The torque versus ROP for the entire test data was fitted with a linear regression line and the slope for each test configuration is plotted in Figure 5.5. (a) and Figure 5.5. (b) for the 4 and 5 bladed bits, respectively. For both bits, it can be seen that the torsional compliance configuration shows the highest slope at each rotational speed test. The effect of the test configuration on the 4-bladed test is significantly higher than the 5-bladed test as indicated by the slope difference between the rigid and the torsional compliance (Figure 5.5.). This is due to the fact that higher ROP was reached with the 4-bladed bit compared to the 5-bladed bit.

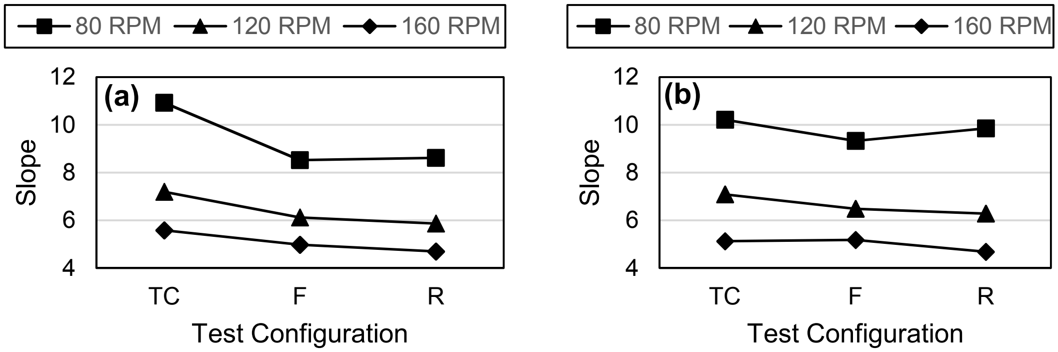


*Figure 5.5. The Slope of the Linear Regression Line of Torque and ROP for (a) 4-Bladed bit, and (b) 5-Bladed bit.*

### 5.2.2 Rigid retest, axial compliance and combined axial-torsional compliance configurations

Linear interpolation was used to calculate the ROP of each test configuration at their respective applied rotational speed for the selected three WOB levels. The selected WOB levels differ from comparison to comparison due to the restriction and misalignment of the available WOB range for the rigid retest, axial, and combined axial-torsional compliance results. The computer controlled rigid retest WOB range sufficiently reaches the WOB ranges of the compliance tests. Although it surpasses the ranges of the axial and combined compliance tests and simultaneously initiates at a higher WOB. Therefore, the lowest WOB data points of the manually controlled rigid retest were included to increase the amount of WOB overlap between the rigid retest and compliance results. For example, the 4-blade PDC, at 160 RPM comparison has the 3 levels at 1800 lb, 2400 lb, and 3000 lb, while the 5-blade PDC, at 120 RPM test has the 3 levels placed at 1900 lb, 2500 lb, and 2800 lb. Figure 5.6 shows the calculated ROP, using linear interpolation, comparison for the 4-blade rigid retest, axial compliance, and combined compliance configurations for all applied rotational speeds.

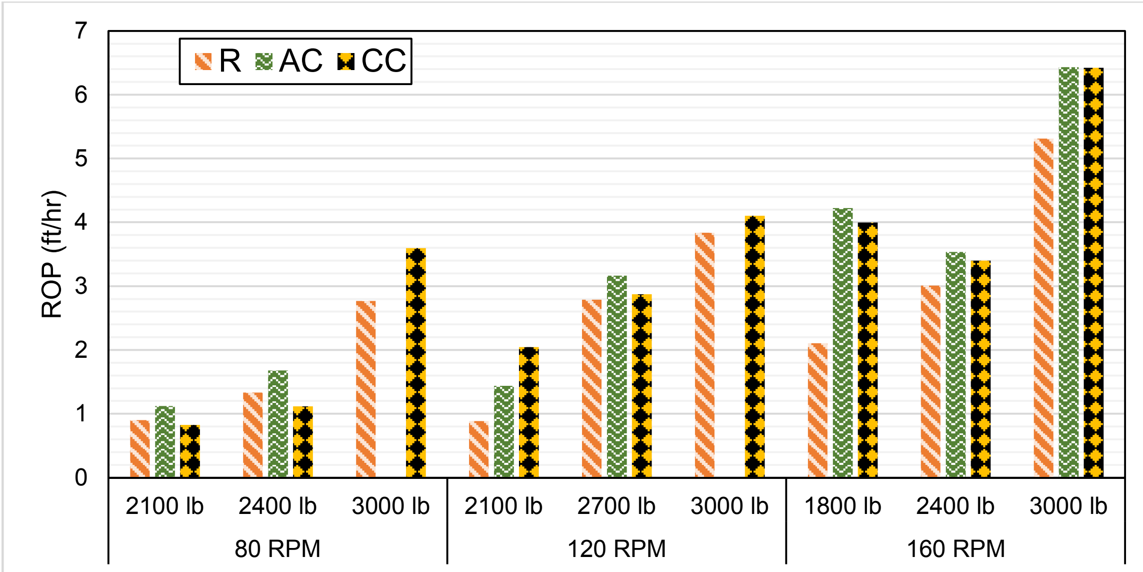


*Figure 5.6. ROP Comparison of Rigid Retest (R), Axial Compliance (AC), and Combined Compliance (CC) Configurations with the 4-Bladed PDC*

The rigid retest values do not begin to see increased ROPs until above the maximum WOB threshold of the compliance tests in all RPM ranges, and thus in the results shown in Figure 5.6, the retest consistently produces lower ROP values than both the axial and combined compliance testing. Since the rigid retest results (Figure 4.7) reach 10 ft/hr at 4500 lb WOB is reached for all RPMs, the compliance of the two compliant drillstrings may be facilitating bit rock interaction at low WOB values that the rigid drillstring will not allow, similar to what is seen in the rigid-torsional compliance comparison at low WOB (Figure 4.6). Another consistent result is better drilling performance from the axial compliance configuration than the combined compliance configuration by a margin of 5-20%, however, as RPM increases, the margin of difference between the axial and combined compliance configurations decreases.

The 5-blade PDC (Figure 5.7) results show similar results to the 4-blade ROP comparison. Although in a set of tests, the axial compliance test had significantly higher ROP than in the 4-blade tests, but still maintains a relationship of being consistently higher than the combined compliance results. For the 5-blade PDC, the axial compliance configuration produces 17%, 38%, and 65% higher ROPs than the combined compliance configuration at 80, 120, and 160 RPM, respectively. The axial compliance results are also higher than the rigid retest results at low WOB, with the only exception being the 80 RPM, 4500 lb data point, where the rigid retest result surpasses the axial compliance result in magnitude, providing a further argument that the compliant drillstring configurations are performing better at low WOB values.

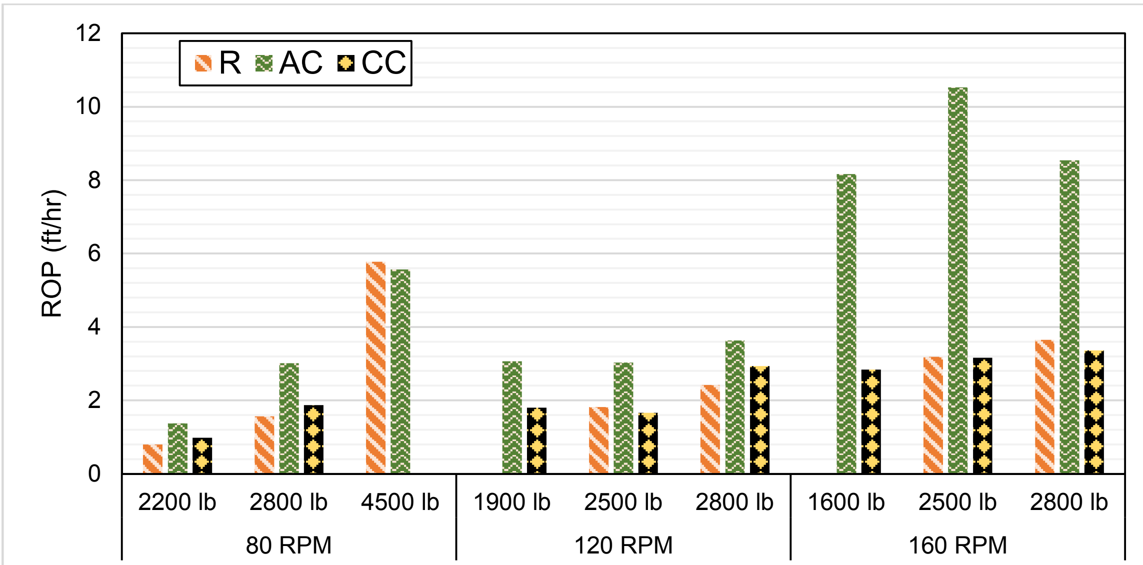


*Figure 5.7. ROP Comparison of Rigid Retest (R), Axial Compliance (AC), and Combined Compliance (CC) Configurations with the 5-Bladed PDC*

Figure 5.4. shows the torque versus ROP for the 4-bladed bit at 80 RPM for the rigid retest, axial compliance, and combined compliance drilling configurations. Again, a linear line is fitted which describes the amount of torque required to produce a given ROP based on the test configuration. The higher the slope of the line fit the more torque is required to achieve a certain ROP. The reduced WOB range makes interpretation of this graph for the compliance configurations difficult, but upon close inspection the axial compliance trendline appears to have the highest slope, indicating a higher torque required to achieve the same ROP than the rigid retest or combined compliance

configurations. The combined compliance and rigid retest configurations are similar in slope, though the rigid retest results in lower torque values required to achieve a given ROP.

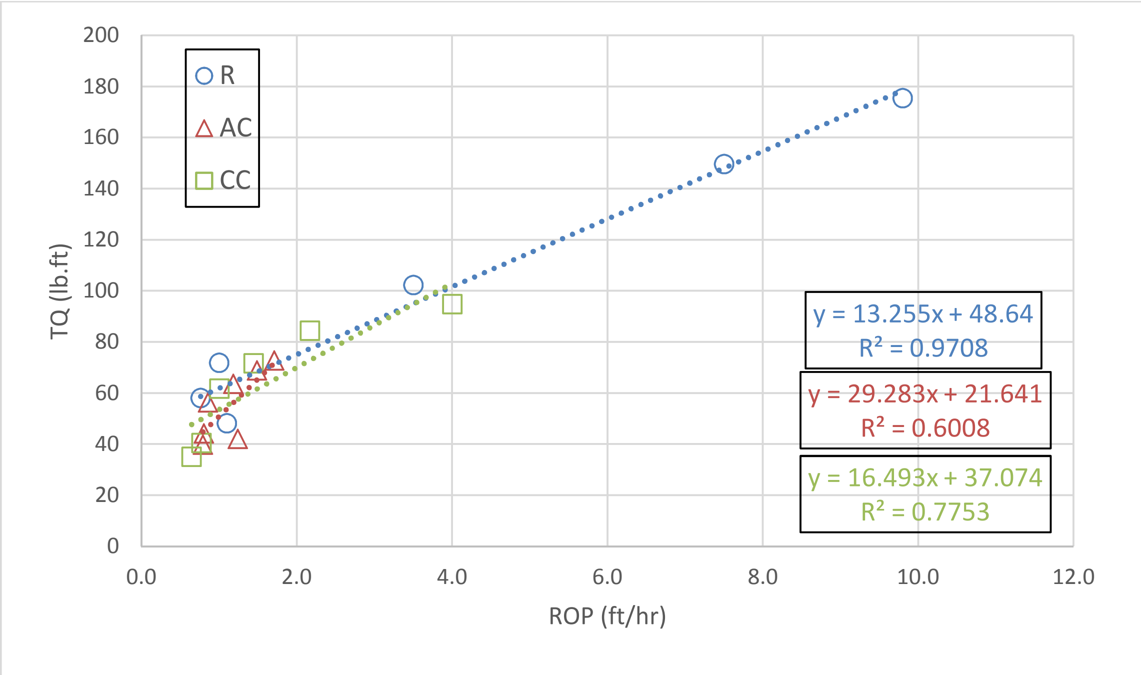


*Figure 5.8. Torque vs. ROP at 80 RPM for the 4-bladed PDC Bit with Rigid Retest (R), Axial Compliance (AC), and Combined Compliance (CC) Configurations*

The torque versus ROP for the test data was fitted with a linear regression line, and the slope for each test configuration is plotted in Figure 5.5. (a) and Figure 5.5. (b) for the 4 and 5 bladed bits, respectively. For both bits, it can be seen that the axial compliance configuration shows the highest slope at each rotational speed test, except in the 5-blade, 160 RPM configuration where the slope is negative. This is due to the erratic nature of the resultant data that can be seen in Figure 4.11 (c) and (f). For the 4-blade PDC, the slope of the rigid retest and combined compliance tests are similar. The combined compliance slope is higher at the 80 and 120 RPM tests, while the rigid retest slope is slightly higher at 160 RPM. For the 5-blade PDC, this relationship is inverted, with the combined compliance having a higher slope only at 160 RPM, while the rigid retest is higher in the 120 RPM test, and significantly higher at 80 RPM. This could be due to the aggressive nature of the bit having more effect on the bit-rock interaction at low RPMs in the rigid drillstring.

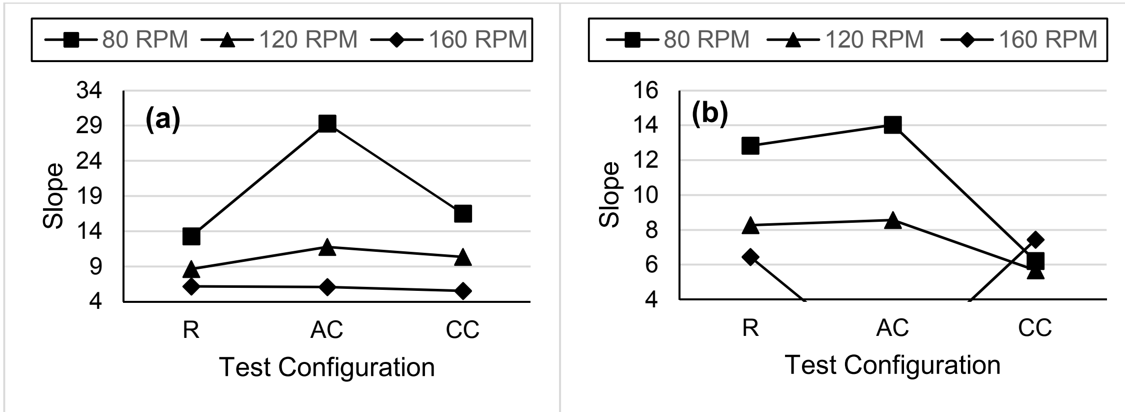


*Figure 5.9. The Slope of the Linear Regression Line of Torque and ROP for (a) 4-Bladed bit, and (b) 5-Bladed Bit.*

CHAPTER VI

# 6 CONCLUSIONS

Drill bit laboratory testing is most commonly performed with a rigid configuration, which does not accurately reflect the actual field conditions and performance seen in field applications. The results indicate that drillstring vibrations have an impact on drill bit performance. This implies that drillstring vibration modes directly affect drilling performance and it is not just a function of bit design. While drillstring vibrations are very complex due to the nature of the problem, the natural vibrations frequencies of the drillstring can be adjusted by reconfiguration of the bottom hole assembly and stabilizers placements to control the effect of drillstring vibrations on ROP.

In the case of torsional vibrations, conventional laboratory testing overestimates bit performance by 35% in the case of hard rock geothermal drilling, although the torsional compliance configuration produces more stable torque than the rigid configuration, which facilitates imporved performance in phase I drilling.

Based on the available data from the rigid retests and the axial compliance configurations, it seems that until a WOB threshold is reached at approximately 4500 lb, the axial compliance facilitates a level of bit-rock interaction that allows for improved performance over the rigid drillstring. However, once that 4500 lb WOB is surpassed, the ROP for the rigid drillstring significantly overtakes the recorded axial values. The inclusion of the torsional compliance in the combined configuration resulted in a 5-20% performance detriment for the 4-blade testing, and a rapidly increasing, up to 65%, detriment for the 5-blade testing relative to the axial compliance configuration.

REFERENCES


Akhtarmanesh, S., Atashnezhad, A., Hareland, G., and Al Dushaishi, M. 2021. ROP Model for PDC Bits in Geothermal Drilling. Presented at the 55th U.S. Rock Mechanics/Geomechanics Symposium, virtual, June. Paper No. ARMA-2021-1214.

Akutsu, E., Mads Rodsjo, D., Gjertsen, J., Andersen, M., Reimers, N., Granhoy-Lieng, T.M., Strom, E., and Horvei, K.A. 2015. Faster ROP in Hard Chalk: Proving a New Hypothesis for Drilling Dynamics. Presented at the SPE/IADC Drilling Conference and Exhibition. London, United Kingdom, March 17-19. https://doi.org/10.2118/173068-MS.

Albdiry, M.T., and Almensory, M.F. 2016. Failure Analysis of Drillstring in Petroleum Industry: A Review. Engineering Failure Analysis. Vol. 65, pp. 74-85. https://doi.org/10.1016/j.engfailanal.2016.03.014.

Al-Enezi, D., Gholoum, S., Al-Hajeri, M., Mohammed, J., Al-Enezi, R., Deori, R., Pandya, M., Omar, M., Agawani, W., Valbuena, F., and Abdelhamid, A. 2018. Middle East Success Story with World's First Adaptive Drill Bit and Premium Rotary Steerable Technology. Presented at the SPE Asia Pacific Oil and Gas Conference and Exhibition. Brisbane, Australia, October 23-25. https://doi.org/10.2118/191869-18APOG-MS.

Al Dushaishi, M., Nygaard, R., Andersen, M., Jeffery, C., Hellvik, S., Saasen, A., and Hareland, G. 2016. Selecting Optimum Drilling Parameters by Incorporating Vibration and Drilling Efficiency Models. Presented at the IADC/SPE Drilling Conference and Exhibition. Fort Worth, Texas, USA. March 1-3. https://doi.org/10.2118/178834-MS.

Alwaar, A., Abugharara, A. N., and and Butt, S. 2018. PFC-2D Numerical Study of the Influence of Passive Vibration Asisted rotary Drilling Tool (pVARD) on Drilling Performance Enhancement. Proceedings of the ASME 37th International Conference on Ocean, Offshore and Arctic Engineering. Madrid, Spain, June 17-22. https://doi.org/10.1115/OMAE2018-78057.

Arevalo, Y., and Fernandes, A. 2012. Quantification of Drillstring-Integrity-Failure Risk Using Real-Time Vibration Measurements. SPE Drilling and Completion. Vol. 27(02), pp. 216-222. https://doi.org/10.2118/147747-PA.

Ashley, D. K., McNary, X. M., and Tomlinson, J. C. 2001. Extending BHA Life with Multi-Axis Vibration Measurements. Presented at the SPE/IADC Drilling Conference, 27 February – 1 March, Amsterdam, Netherlands. https://doi.org/10.2118/67696-MS.

Atashnezhad, A., Akhtarmanesh, S., Hareland, G., and Al Dushaishi, M. 2021. Developing a Drilling Optimization System for Improved Overall Rate of Penetration in Geothermal Wells. Presented at the 55th U.S. Rock Mechanics/Geomechanics Symposium, 20-23 June, Houston, TX. Paper No. ARMA-21-1215.

Atashnezhad, A., Akhtarmanesh, S., Sleeper, S., and Hareland, G. 2020. Rate of Penetration (ROP) Model for PDC Drill Bits based on Cutter Rock Interaction. In 54th US Rock Mechanics/Geomechanics Symposium. American Rock Mechanics Association. 28 June-1 July, Golden, Colorado, USA.Babatunde, Y., Butt, S., Molgaard, J., and Arvani, F. 2011. Investigation of the Effects of Vibration Frequency on (a) (b) Rotary Drilling Penetration Rate Using Diamond Drag Bit. Presented at the 45th US Rock Mechanics/Geomechanics Symposium, 26-29 June, San Francisco, CA.

Barnett, L., Klein, K., Al Dushaishi, M. F., Nygaard, R., and Hareland, G. 2021. Field Data Analysis and Modeling of Drillstring Vibrations to Identify Inefficiency in Deep Geothermal Drilling. Presented at the 55th US Rock Mechanics/Geomechanics Symposium, 20-23 June, Houston, TX. Paper No. ARMA-21-2015

Clausen, J.R., Schen, A.E., Forster, I., Prill, J., and Gee, R. 2014. Drilling with Induced Vibrations Improves ROP and Mitigates Stick/Slip in Vertical and Directional Wells. Presented at the IADC/SPE Drilling Conference and Exhibition. Fort Worth, Texas, USA. March 4-6. https://doi.org/10.2118/168034-MS.

Dunayevsky, V.A., Abbassian, F., and Judzis, A. 1993. Dynamic Stability of Drillstrings Under Fluctuating Weight on Bit. SPE Drilling and Completion. Vol. 8(02) pp. 84-92. https://doi.org/10.2118/14329-PA.

Dunayevsky, V.A., and Abbassian, F. 1998. Application of Stability Approach to Bit Dynamics. SPE Drilling and Completion. Vol. 13(02) pp. 99-107. https://doi.org/10.2118/30478-PA.

Dupriest, F., and Koederitz, W. 2005. Maximizing Drill Rates with Real-time Surveillance of Mechanical Specific Energy. Presented at the SPE/IADC Drilling Conference. February, Amsterdam, Netherlands. https://doi.org/10.2118/92194-MS.

Elsayed, M.A., and Raymond, D.W. 2002. Analysis of Coupling Between Axial and Torsional Vibration in a Compliant Model of a Drillstring Equipped with a PDC Bit. Presented at the ASME Engineering Technology Conference on Energy. Texas, USA. February 4-5. https://doi.org/10.1115/ETCE2002/STRUC-29002.

Feauto, B.I., Jeffery, C., Hanley, C., and Duff, R.G. 2013. Drilling Assembly Vibration Model Validated with Frequency Domain Examination of Distributed Downhole Measurements. Presented at the SPE Middle East Intelligent Energy Conference and Exhibition. Manama, Bahrain. October 28-30. https://doi.org/10.2118/167466-MS.

Finger, J.T. and Blankenship, D.A., 2012. Handbook of best practices for geothermal drilling (No. SAND2011-6478). Sandia National Lab. (SNL-NM), Albuquerque, NM (United States).

Garcia-Gavito, D., and Azar, J.J. 1994. Proper Nozzle Location, Bit Profile, and Cutter Arrangement Affect PDC-Bit Performance Significantly. SPE Drilling and Completion. Vol. 9(03), pp. 167-175. https://doi.org/10.2118/20415-PA.

Glowka, D.A., and Stone, C.M. 1985. Thermal Response of Polycrystalline diamond Compact Cutters Under Simulated Downhole Conditions. Society of Petroleum Engineers Journal. Vol. 25(02), pp. 143-156. https://doi.org/10.2118/11947-PA.

Hareland, G., Nygaard, R., Yan, W., and Wise, J.L. 2009. Cutting Efficiency of a Single PDC Cutter on Hard Rock. Journal of Canadian Petroleum Technology. Vol. 48(06), pp. 60-65. https://doi.org/10.2118/09-06-60.

Hareland, G., and Rampersad, P.R. 1994. Drag-Bit Model Including Wear. Presented at the III Latin American/Caribbean Petroleum Engineering Conference. 27-29 April, Buenos Aires, Argentina.

International Association of Drilling Contractors (IADC). 2014. IADC Drilling Manual, $12^{th}$ Edition. IADC, Houston, TX.

Kerkar, P. B., Hareland, G., Fonseca, E. R., and Hackbarth, C. J. 2014. Estimation of rock compressive strength using downhole weight-on-bit and drilling models. Presented at the International Petroleum Technology Conference. Doha, Qatar. January 20-22.

Ledgerwood III, L.W., Jain, J. R., Olivier, H. J., and Spencer, R. W. 2013. Downhole Measurement and Monitoring Lead to an Enhanced Understanding of Drilling Vibrations and Polycrystalline Diamond Compact Bit Damage. SPE Drill & Compl 28(3): 254–262. https://doi.org/10.2118/134488-PA.

Li, H., Butt, S., Munaswamy, K., and Arvani, F. 2010. Experimental Investigation of Bit Vibration on Rotary Drilling Penetration Rate. Presented at the 44th U.S. Rock Mechanics Symposium. Salt Lake City, Utah, USA. June 27-30.

Makkar, N., Sullivan, E., and Habernal, J. 2014. Coupling Between Lateral and Torsional Vibrations: A New Insight into PDC Bit Drilling Inefficiencies. Presented at the Offshore Technology Conference-Asia, Kuala Lumpur, Malaysia, March 25–28. https://doi.org/10.4043/25056-MS.

Miyazaki, K., Ohno, T., Karasawa, H., and Imaizumi, H. 2019. Performance of Polycrystalline Diamond Compact Bit Based on Laboratory Tests Assuming Geothermal Well Drilling. Geothermics, pp. 185-194. https://doi.org/10.1016/j.geothermics.2019.03.006.

Motahhari, H. R., Hareland, G., and James, J. A. 2010. Improved drilling efficiency technique using integrated PDM and PDC bit parameters. In Journal of Canadian Petroleum Technology, 49(10), 45-52. SPE-141651-PA.

Rafatian, N., Miska, S., Ledgerwood, W., Ahmed, R., Yu, M. and Takach, N. 2010. Experimental study of MSE of a Single PDC Cutter Interacting with Rock Under Simulated Pressurized Conditions. SPE Drilling & Completion Journal. Vol. 25(01). https://doi.org/10.2118/119302-PA.

Rahmani, R., Pastusek, P., Yun, G., Roberts, T. 2020. Investigation of Geometry and Loading Effects on PDC Cutter Structural Integrity in Hard Rocks. Presented at the IADC/SPE International Drilling Conference and Exhibition. Texas, USA. March 3-5. https://doi.org/10.2118/199598-MS.

Rajabov, V., Miska, S., Mortimer, L., Yu, M. and Ozbayoglu, E. 2012. The Effects of Back Rake and Side Rake Angles on Mechanical Specific Energy of Single PDC Cutters with Selected Rocks at Varying Depth of Cuts and Confining Pressure. Presented at the IADC/SPE Drilling Conference and Exhibition. San Diego, California, USA. March 2012. https://doi.org/10.2118/151406-MS.

Raymond, D.W., 2001. PDC bits demonstrate benefit over conventional hard-rock drill bits. TransactionsGeothermal Resources Council, pp. 125-132

Raymond, D. W., Elsayed, M. A., Polsky, Y., and Kuszmaul, S. S. 2008. Laboratory simulation of drill bit dynamics using a model-based servohydraulic controller. Journal of Energy Resources Technology. Vol. 130(4). https://doi.org/10.1115/1.3000142.

Raymond, D., Knudsen, S., Blankenship, D., Bjornstad, S., Barbour, J., and Schen, A. 2012. PDC Bits Outperform Conventional Bit in Geothermal Drilling Project, GRC Resources Council Transactions, v.6, p.307-315.

Rivas, M., Ramirez, A., Al-Zahrani, B., and Abouelnaaj, K. 2021. Mitigating Twist-Offs While Drilling with the Help of BHA Dynamics Software. Presented at the SPE/IADC Middle

East Drilling Technology Conference and Exhibition. Abu Dhabi, UAE. May 25-27. https://doi.org/10.2118/202174-MS.

Soares, C., Daigle, H., and Gray, K. 2016. Evaluation of PDC Bit ROP Models and the Effect of Rock Strength on Model Coefficients. Journal of Natural Gas Science and Engineering. Vol. 34 pp. 1225-1236.

Teale, R. 1965. The Concept of Specific Energy in Rock Drilling. International Journal of Rock Mechanics, 2(1), pp. 57-73. https://doi.org/10.1016/0148-9062(65)90022-7.

Vromen, T., Detournay, E., Nijmeijer, H., and Van de Wouw, N. 2019. Dynamics of Drilling Systems With an Antistall Tool: Effect on Rate of Penetration and Mechanical Specific Energy. Society of Petroleum Engineers Journal. Vol. 24(05). https://doi.org/10.2118/194487-PA.

Warren, T.M., and Oster, J.H. 1998. Torsional Resonance of Drill Collars with PDC Bits in Hard Rock. Presented at the SPE Annual Technical Conference and Exhibition. New Orleans, Louisiana, USA. September 27-30. https://doi.org/10.2118/49204-MS.

Wise, J.L., Raymond, D.W., Cooley, C.H. and Bertagnolli, K., 2002. Effects of design and processing parameters on performance of PDC drag cutters for hard-rock drilling. Transactions-Geothermal Resources Council, pp.201-206.

Wise, J.L., Mansure, A.J. and Blankenship, D.A., 2005. Hard-Rock Field Performance of Drag Bits and a Downhole Diagnostics-While-Drilling (DWD) Tool. GRC Transactions, 29.

VITA

Laymon Barnett

Candidate for the Degree of

Master of Science

Thesis: LABORATORY SCALE EVALUATION OF COMPLIANT DRILLSTRING WITH PDC BITS IN GEOTHERMAL APPLICATIONS

Major Field: Petroleum Engineering

Biographical:

Education:

Completed the requirements for the Master of Science in Petroleum Engineering at Oklahoma State University, Stillwater, Oklahoma in May 2022.

Completed the requirements for the Bachelor of Science in Biosystems Engineering at Oklahoma State University, Stillwater, Oklahoma in 2018.

Experience:
1 year Roustabout/Safety Supervisor at Top Hand Field Services
3 months Floorhand at Cactus Drilling
1 year 2 months Measurements Field Engineer at Schlumberger
3 months Reservoir Engineering Intern at Ascent Resources
2 years Graduate Research Assistant at Oklahoma State University

Professional Memberships:
Society of Petroleum Engineers
American Association of Drilling Engineers